ISOCHRONAL HYDROGENATION OF TEXTURED MAGNESIUM/PALLADIUM THIN FILMS

A THESIS SUBMITTED TO
THE GRADUATE SCHOOL OF NATURAL AND APPLIED SCIENCES
OF
MIDDLE EAST TECHNICAL UNIVERSITY

BY

ÇAĞLA ÖZGİT

IN PARTIAL FULFILLMENT OF THE REQUIREMENTS
FOR
THE DEGREE OF MASTER OF SCIENCE
IN
METALLURGICAL AND MATERIALS ENGINEERING

FEBRUARY 2009

Approval of the thesis:

ISOCHRONAL HYDROGENATION OF TEXTURED MAGNESIUM/PALLADIUM THIN FILMS

submitted by **ÇAĞLA ÖZGİT** in partial fulfillment of the requirements for the degree of **Master of Science in Metallurgical and Materials Engineering Department, Middle East Technical University** by,

Prof. Dr. Canan Özgen
Dean, Graduate School of **Natural and Applied Sciences** _____

Prof. Dr. Tayfur Öztürk
Head of Department, **Metallurgical and Materials Engineering** _____

Prof. Dr. Tayfur Öztürk
Supervisor, **Metallurgical and Materials Engineering Dept., METU** _____

Examining Committee Members:

Prof. Dr. Macit Özenbaş
Metallurgical and Materials Engineering Dept., METU _____

Prof. Dr. Tayfur Öztürk
Metallurgical and Materials Engineering Dept., METU _____

Prof. Dr. Vedat Akdeniz
Metallurgical and Materials Engineering Dept., METU _____

Prof. Dr. Mehmet Parlak
Department of Physics, METU _____

Assoc. Prof. Dr. Caner Durucan
Metallurgical and Materials Engineering Dept., METU _____

Date: 10.02.2009

I hereby declare that all information in this document has been obtained and presented in accordance with academic rules and ethical conduct. I also declare that, as required by these rules and conduct, I have fully cited and referenced all material and results that are not original to this work.

Name, Last Name : Çağla Özgit

Signature :

ABSTRACT

ISOCHRONAL HYDROGENATION OF TEXTURED MAGNESIUM/PALLADIUM THIN FILMS

Özgit, Çağla

M.Sc., Department of Metallurgical and Materials Engineering

Supervisor: Prof. Dr. Tayfur Öztürk

February 2009, 78 pages

Pure and palladium-covered 350 nm thick magnesium thin films were deposited on glass substrates via thermal evaporation. In the as-deposited state, films were highly textured with Mg (001) parallel to the substrate. Hydrogen loading experiments were carried out in two different conditions; namely isothermal and isochronal. Hydrogenation behaviors of the thin films were followed by two-point probe electrical resistance and optical transmittance measurements, as well as x-ray diffraction studies. Isothermal hydrogenation experiments conducted on Pd-covered Mg thin films have revealed that these films can absorb hydrogen at temperatures starting from 333 K, producing MgH_2 with a random texture. When the films were heated slowly starting from the room temperature, on the other hand, hydrogenation gives rise to a textured MgH_2, where (110) parallel to the substrate with a minor (101) component. Formation of the textured hydride in isochronal loading was discussed within the context of lattice mismatch in Mg to MgH_2 transformation. It was further shown that formation of such a textured hydride in Mg thin films minimizes in-plane lattice distortion.

Keywords: Magnesium; Magnesium hydride; Hydrogen absorption; Lattice mismatch; Textured thin film.

ÖZ

DOKULU MAGNEZYUM/PALADYUM İNCE FİLMLERDE
HİDRÜR OLUŞUMU

Özgit, Çağla

Y. Lisans, Metalurji ve Malzeme Mühendisliği Bölümü

Tez Yöneticisi: Prof. Dr. Tayfur Öztürk

Şubat 2009, 78 sayfa

350 nm kalınlığındaki saf ve paladyum kaplı magnezyum ince filmler cam altlıklar üzerine ısıl buharlaştırma yöntemi ile çöktürülmüştür. Filmlerin Mg (001) düzlemi cam altlığa parallel olacak şekilde dokulu bir yapıda oldukları gözlemlenmiştir. Hidrürleme deneyleri eşısıl ve eşsüreli olmak üzere iki farklı koşulda gerçekleştirilmiştir. Hidrür oluşumu elektriksel direnç ve optik geçirgenlik ölçümlerine ilave olarak x-ışınları kırınımı ile de takip edilmiştir. Yapılan deneyler, 333 K'den başlayan sıcaklıklarda eşısıl hidrürleme sonucu Mg filmlerin dokusuz MgH_2'ye dönüştüğünü göstermektedir. Öte yandan, aynı filmler eşsüreli koşulda hidrürlendiği taktirde MgH_2'nin dokulu olduğu tespit edilmiştir. (110) düzleminin cam altlığa paralel olarak yönlendiği bu dokuda, az olmakla beraber (101)'in de mevcut olduğu gözlenmiştir. Eşsüreli hidrürleme sonucu görülen bu dokulu yapı, Mg-MgH_2 dönüşümünde gerçekleşen kafes uyuşmazlığı esas alınarak irdelenmiş ve dokunun düzlem içi boyutsal uyumsuzluğu en aza indirgediği gösterilmiştir.

Anahtar Kelimeler: Magnezyum; Magnezyum hidrür; Hidrojen emilimi; Kafes uyuşmazlığı; Dokulu ince film.

in memory of my grandfather

Hasan Tahsin Özgit

(1930 – 2006)

ACKNOWLEDGEMENTS

I would like to express my deepest gratitude and appreciation to my supervisor Prof. Dr. Tayfur Öztürk for his invaluable guidance, endless support and motivation throughout this study.

I am indebted, in an alphabetical order, to Prof. Dr. M. Kadri Aydınol, Assist. Prof. Dr. F. Arcan Dericioğlu, Assoc. Prof. Dr. Caner Durucan, Prof. Dr. Macit Özenbaş, Prof. Dr. Naci Sevinç and Cengiz Tan for the illuminating discussions we had.

I gratefully acknowledge Necmi Avcı, Özdemir Dinç, İsa Hasar, Yaşar Kazanç, Atalay Özdemir and Cemal Yanardağ for their willingness to help whenever I needed. I would also like to thank my friend Emre Yeğin for his generous help in the engineering drawings.

I was lucky to be able to associate myself with the talented and hard working members of Metal-Hydrogen Research Group: Hasan Akyıldız, Gülhan Çakmak, Rabia Ölmez, Taylan Örs, Semra Tan and Serdar Tan. Thank you for your generous help in the experimental phase of this research. I could not have wished for better collaborators.

My warmest thanks to my friends Betül Akköprü, Ergin Büyükakıncı, Arda Çetin, Ali Erdem Eken, Metehan Erdoğan, Emre Ergül, Volkan Kalem, Volkan Kayasü, Alper Kınacı, Güher Kotan, Pelin B. Maradit, Onur Önder, Fatih G. Şen, Elvan Tan and Evren Tan for just being around and bringing joy to my daily routine.

I would also like to express my sincere gratitude to my dearest friends F. Sedef Çift, Damla Işıklılar, Galena İş, E. Ayşe Özşuca, M. Serkan Şahin, L. Özgecan Ulak and Görkem P. Yılmaz for all the things we shared and the moments we spent together.

My special thanks go to my dear friend Deniz Keçik for her continuous encouragements and sincere belief in me. Without your guidance and suggestions this M.Sc. thesis would not have been written.

I am also deeply indebted to Barış Akgün, not only for the joy he brought to my life but also for the help and inspiration he extended.

I would like to acknowledge and extend my heartfelt gratitude to my parents Oya Aytaç and Attila Özgit for their continuous encouragements and support. Last but not least, I would like to thank all my family members, particularly to my grandparents Mübeccel Aytaç, Fethi Aytaç and Özay Özgit. Their care and love enabled me to complete this work.

The research in this dissertation has been supported by the Scientific Research Projects Fund of Graduate School of Engineering (Grant #BAP-2006-07-02-00-01).

TABLE OF CONTENTS

LIST OF TABLES

TABLES

LIST OF FIGURES

FIGURES

CHAPTER 1

INTRODUCTION

With a high gravimetric storage capacity of 7.6 wt.% hydrogen and low cost, magnesium is a promising candidate for hydrogen storage applications. However, its high stability and sluggish reaction kinetics obstruct its widespread use. Although considerable progress has been made in accelerating the reaction rates, the high stability of MgH_2 is still needed to be reduced. Several attempts have been made in order to destabilize this hydride by mainly following the powder-processing routes. Aiming the same goal, thin film processing has been recently emerged as an alternative method for producing nano-sized structures with well controlled chemical make-up and morphology. Furthermore, thin film systems are also known to be advantageous due to their large surface-to-volume ratio, ease of catalyst introduction in systems and better heat transfer arrangements.

Magnesium films reported in the literature were mostly covered by a thin layer of palladium in order to protect the underlying film against oxidation as well as promoting hydrogen dissociation at the surface. Extensive work on these thin films has revealed that temperatures required for hydrogen sorption can be significantly reduced. It has been further shown that both absorption and desorption are possible at temperatures as low as room temperature. However,

studies on Mg thin films are still lacking in terms of correlating the structural properties with their hydrogenation behavior.

In the current study, hydrogenation behavior of Pd-covered Mg thin films deposited on a glass substrate with a strong texture was investigated. Conversion of these films to MgH_2 was examined under both isothermal and isochronal hydrogenation conditions.

Following this brief introduction, in Chapter 2, a literature review on the hydrogen sorption behavior of magnesium thin films – including the details of Mg to MgH_2 phase transition, thermodynamics and kinetics of hydrogen uptake, optical switching upon hydrogenation – is presented. Chapter 3 reports the experimental details on deposition, hydrogenation and characterization of the thin film samples. Here, a short section is dedicated to the design of a custom-made resistance measurement set-up. In Chapter 4, experimental results are given and discussed in detail. At the beginning of that chapter, a comparative study is presented, in which the data obtained from two-point probe electrical resistance and optical transmittance measurement techniques are questioned in terms of how well they represent the amount of MgH_2 formed in the samples. Following this, hydrogenation behaviors of pure and Pd-covered textured Mg thin films are reported for isothermal and isochronal conditions. Moreover, different orientations of the nucleating MgH_2 phase in the case of different hydrogenation conditions are also shown and discussed in detail in terms of lattice mismatch calculations. Conclusions are finally given in Chapter 5.

CHAPTER 2

LITERATURE REVIEW

During the last few decades hydrogen attracted worldwide interest as the rapidly diminishing non-renewable energy resources and greater environmental awareness give rise to the need for more efficient and environmentally friendly fuels. The main problem of using hydrogen as an energy carrier for commercial applications lies in economical and convenient storage. Hydrogen can be stored in the form of gas, liquid or solid (i.e. metal hydride). Among these, metal hydrides received considerable attention since the hydrogen can be stored safely inside the metal itself and the amount of hydrogen stored per volume is greater than either gaseous or liquid storage as emphasized by Ivey and Northwood (1983).

With a high gravimetric storage capacity of 7.6 wt.% hydrogen and low cost, magnesium is a promising candidate for hydrogen storage applications. However, there are several thermodynamic and kinetic limitations preventing its use in industrial applications.

The most significant thermodynamic drawback is the high desorption temperature of ~623 K, which is related to the high stability of the Mg–H bonds in MgH_2 (Buschow *et al.*, 1982). The other drawback is slow hydrogen absorption/desorption kinetics. Paillier *et al.* (2006) have attributed the slow

kinetics as being the result of: (i) presence of a native surface oxide preventing the access of hydrogen to metallic magnesium, (ii) high energy barrier for H_2 dissociation on Mg, and (iii) slow hydrogen diffusion through the MgH_2.

2.1 Hydrogen Sorption in Magnesium Thin Films

The main benefits of thin film metal hydrides can be summarized as follows: (i) thin films provide large surface area with fast charging/discharging rate for hydrogen, (ii) pulverization is slower, (iii) both critical pressure and critical temperature are significantly lower, (iv) they provide better heat transfer arrangements, and (v) protective surface coating could be carried out with ease to stop poisoning by oxygen and activation of thin film hydrides is possible by coating them with a thin layer of catalytic material (Jain *et al.*, 1988). In the light of these advantages, numerous studies were undertaken concerning hydrogen storage in magnesium thin films.

The first study reporting the hydrogen sorption behavior of Pd-covered Mg thin films was published by Krozer and Kasemo in 1987. They observed unusual kinetics in their study: (i) the hydrogen uptake saturated far from MgH_2 at room temperature, and (ii) the saturation uptake decreased with increasing H_2 pressure. They explained their results in terms of a hydride formation at the Pd/Mg interface, which blocks hydrogen diffusion. Two years later, Rydén *et al.* (1989) verified and investigated the existence of this interface hydride by applying hydrogen depth profiling. In their study, Rydén *et al.* (1989) concluded that there is a significant thermodynamic driving force for the interface hydride formation.

In 1989, Krozer and Kasemo measured the hydrogen equilibrium uptake and associated kinetics of magnesium films in the temperature range 260-360 K and pressure range 0.03-30 Torr, and demonstrated that equilibrium can be established between H_2 gas and magnesium at much lower pressures and temperatures than previously reported, by the use of thin, UHV-prepared and palladium-coated samples. Here, Krozer and Kasemo used a thin palladium overlayer for (i) its catalytic effect on H_2 dissociation, (ii) its increase of the hydrogen sticking coefficient, and (iii) its effective protection against oxidation in the case of exposure of samples to air. Just a year later, in 1990, Krozer and Kasemo published another article, in which they reviewed all their experimental data on the hydrogen sorption characteristics of the thin film Mg–H system.

Hjort *et al.* (1996a) performed resistivity measurements during hydriding-dehydriding cycles of UHV-prepared Mg films. This was the first study in which electrical resistivity (or resistance) measurements were used to follow hydrogen concentration in Mg thin film samples. In their study, resistivity versus hydrogen concentration relation was found to be linear up to $x = (H/Mg)$ *(atom ratio)* ≈ 0.4 according to the formula $\rho(x) = \rho(0)\,(1 + c \cdot x)$, where ρ is the resistivity and $c = 1.08 \pm 0.25$. Hjort *et al.* (1996a) further stated that, for $x > 0.4$, the variation of $\rho(x)$ with hydrogen concentration became stronger than linear, but remained still rather weak until x reached values around 1-1.5, where resistivity increased very rapidly by about a factor of 5. In the context of their study, the resistivity data were also compared with those obtained from quartz crystal microbalance (QCM) measurements. As a result, the general behavior obtained with both methods was found to be the same.

In another study, Hjort *et al.* (1996b) investigated the influence of oxygen on the hydrogen uptake by Pd-coated Mg films. As a result of their study, they concluded that oxygen at the Mg/Pd interface has two functions: (i) at low

concentrations its main effect is to accelerate the hydrogen uptake and thereby cause an earlier blocking of the interface, and (ii) at large concentrations the oxygen instead reduces the uptake rate, which prevents total hydride blocking and leads to higher total uptake.

In 1999, Higuchi *et al.* investigated the hydrogen sorption properties of 200 nm thick Mg thin films coated with 25 nm Pd, having different degree of crystallization in the Mg layer. In this study, dehydrogenation temperature was found to become lower as the degree of Mg crystallization decreases. The same group of researchers (Yamamoto *et al.*, 2002) continued their work on Mg thin films, this time, by focusing on the optical and structural properties. In their study, they showed that fully hydrogenated films were in a color-neutral transparent state. In another study (Higuchi *et al.*, 2002), they investigated hydrogen storage properties of three-layered Pd/Mg/Pd films prepared by RF-associated magnetron sputtering method. Their results indicated that the dehydrogenation behavior can be improved significantly by the use of such a three-layered structure.

The hydrogenation characteristics of 30 μm thick air-exposed magnesium thin films were studied by Léon *et al.* (2002). They showed that these films can absorb 7.5 wt.% of hydrogen at 623 K under a hydrogen pressure of 10 bar and desorb all the hydrogen at the same temperature under a hydrogen pressure of 0.21 bar, emphasizing that the hydrogenation-dehydrogenation occurs even though the films were exposed to air. In their following study, Léon *et al.* (2003) investigated the hydrogen sorption properties of vanadium- and palladium-implanted magnesium films. They pointed out that vanadium-implanted films exhibit faster hydrogen absorption compared to pure magnesium and to palladium-implanted films and the (de)hydrogenation kinetics depend on the ion dose implanted.

In 2004, Yoshimura *et al.* reported that magnesium thin films were hydrogenated upon exposure to 4% hydrogen gas diluted by argon at room temperature.

A similar study to that of Hjort *et al.* (1996a) was conducted nine years later by Ingason and Olafsson (2005), in which resistance measurements were done on 100 nm Mg films covered with 10 nm Pd in temperatures ranging from 333 to 373 K. Results obtained from this study showed a thermodynamic behavior similar to that found in bulk magnesium and magnesium-based samples made by ball milling.

Paillier and Roué (2005), on the other hand, studied the structure and electrochemical hydriding behavior of Mg/Pd thin films prepared using pulsed laser deposition (PLD) technique. In their following study, Paillier *et al.* (2006) investigated the influence of the deposition atmosphere on the film morphology and electrochemical hydrogenation characteristics of Mg/Pd thin films elaborated by PLD.

Akyıldız *et al.* (2006) studied on the hydrogenation behavior of Mg based thin films produced via thermal evaporation. Experiments conducted on Au-Pd capped Mg thin films at 473 K revealed that upon exposure to hydrogen gas (P_{H2} = 10 bar) for 1 hour, considerable amount of MgH_2 forms in the film, though some fraction still remains as Mg.

The surface science investigations performed by Ostenfeld and Chorkendorff (2006) implied that the post-oxidizing of Mg films increases the apparent desorption energy from 146 kJ/mol to 314 kJ/mol. The authors also pointed out that magnesium oxide overlayers serve as a cap, preventing magnesium sublimation and delay the hydrogen desorption from the hydride phase.

In another study, Shalaan and Schmitt (2006) investigated the optical and structural properties of Mg nanoparticle thin films coated with Pd. They succeeded to load thin films of Mg with hydrogen at room temperature and normal pressure of hydrogen gas. In their study, transparent MgH_2 was obtained in less than 100 seconds. In the meantime, Pasturel *et al.* (2006) reported that Pd-doped Mg can also absorb hydrogen at room temperature and less than 1 bar pressure in a few minutes.

The influence of oxygen contamination on the hydride formation in Pd-covered thin films of Mg has been studied via resistance measurements by Ingason and Olafsson (2006). Their work showed that the presence of oxygen contamination initially increases the rate of uptake greatly but decreases it when the Mg film is contaminated further with oxygen.

The structural and hydrogen storage properties of nanostructured Pd-capped Mg thin films prepared by two different methods, namely plasma sputter deposition and pulsed laser deposition, were studied by Singh *et al.* (2007). The authors stated that a maximum hydrogen uptake of 4 to 7.5 wt.% is reached under optimum hydrogen loading conditions of pressures between 2.5-10 bar at a temperature of ~470 K for both types of films.

In 2007, Domènech-Ferrer *et al.* showed that nanostructured Mg films can be hydrogenated at temperatures as low as 323 K in few minutes. It was also pointed out that aluminum addition has a beneficial effect on the hydrogenation characteristics of the Mg films, without a significant decrease in the desorption temperature.

In another study, hydrogenation properties of 40 nm thick Mg films, grown under UHV conditions, have been studied at elevated temperatures and

pressures, i.e. conditions relevant for hydrogen storage, by Ostenfeld *et al.* (2007). It has been shown that the addition of a small amount of Pt to the magnesium surface increases the sticking coefficient, whereas decreases the influence of self blocking caused by the adsorbed hydrogen. Ostenfeld *et al.* (2007) further stated that atomic hydrogen diffuses through post-oxidized magnesium oxide films, but not through stoichiometric magnesium oxide.

Kelekar *et al.* (2007), in their study, emphasized that kinetics of hydrogen absorption and desorption depend on the surface orientation and degree of crystallinity of the original magnesium layer. They further pointed out that hydrogen diffusion is an important factor governing the desorption kinetics.

Recently, Qu *et al.* (2009) reported the superior hydrogen sorption properties of Pd-capped Mg thin films. The authors stated that their samples became transparent and insulating after hydrogenation at 353 K and reverted to the metallic mirror state completely and rapidly on exposure to air at 298 K.

2.1.1 Magnesium to Magnesium Hydride Phase Transformation in Thin Films

Metal to metal hydride phase transition in the Mg–H system involves not only substantial volume expansion, but also a structural transformation. Upon hydrogenation, the hexagonal close-packed structure of magnesium metal changes into the tetragonal structure of magnesium hydride, while the overlying palladium lattice retains the same face-centered cubic structure, where hydrogen atoms are located in the interstitial octahedral sites.

X-ray diffraction studies performed on magnesium hydride (MgH_2) by Ellinger *et al.* (1955) revealed that this ionic compound, with an appreciable covalent contribution (Stander and Pacey, 1978), crystallizes in the tetragonal system with

a = 4.5168 ± 0.0005 Å and c = 3.0205 ± 0.0005 Å. Ellinger *et al.* (1955) also reported measured density as 1.45 ± 0.03 g/cm^3, showing that there are two molecules in the unit cell. They further pointed out that two magnesium atoms in the unit cell are in a body-centered configuration, i.e. 2 Mg in (000) (½ ½ ½). Space group of this compound was found to be $P4_2/mnm$ (D_{4h}^{14}) and the positions of the 4 H atoms were given as ± (x, x, 0) (x+½, ½-x, ½) with x = 0.306. Moreover, in this structure, given by Ellinger *et al.* (1955), each magnesium is coordinated to six hydrogens at a distance of 1.95 Å and each hydrogen is coordinated to three magnesiums. One H-H distance is 2.49 Å and the others are 2.76 Å.

Since the hydrogen atoms had no measurable effect on the diffraction intensities, there was no experimental proof for the hydrogen positions proposed by Ellinger *et al.* (1955). In this respect, a direct determination of the hydrogen sites by means of neutron diffraction was undertaken by Zachariasen *et al.* (1963), using the deuteride in preference to the hydride. As a result of their work, hydrogen positions within the tetragonal MgH_2 compound were identified, i.e. x = 0.306 ± 0.003. The unit cells of hexagonal close-packed magnesium and tetragonal (rutile-type) magnesium hydride are shown schematically in Figure 2.1(a) and (b), respectively.

The nature of Mg to MgH_2 transformation has been the subject of several investigations. In 1981, Schöber studied the exothermic formation of MgH_2 in Mg by transmission electron microscopy (TEM). The sample investigated was high purity magnesium foil hydrogenated at 543 K for about 16 hours under a hydrogen pressure of 50 bar. The morphology and also the crystallography observed in this TEM work was representative of bulk. The orientation relationship between Mg and the nucleating MgH_2 phases was found to be as Mg (001) // MgH_2 (100) and Mg [110] // MgH_2 [001] as demonstrated in Figure 2.2, from the selected area diffraction patterns (SAD) showing both phases.

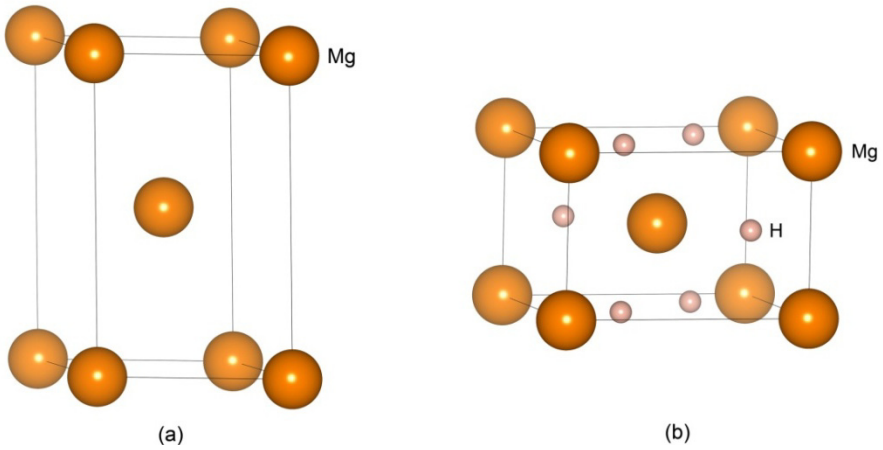

Figure 2.1 The representative unit cells of (a) hexagonal close-packed magnesium and (b) tetragonal magnesium hydride.

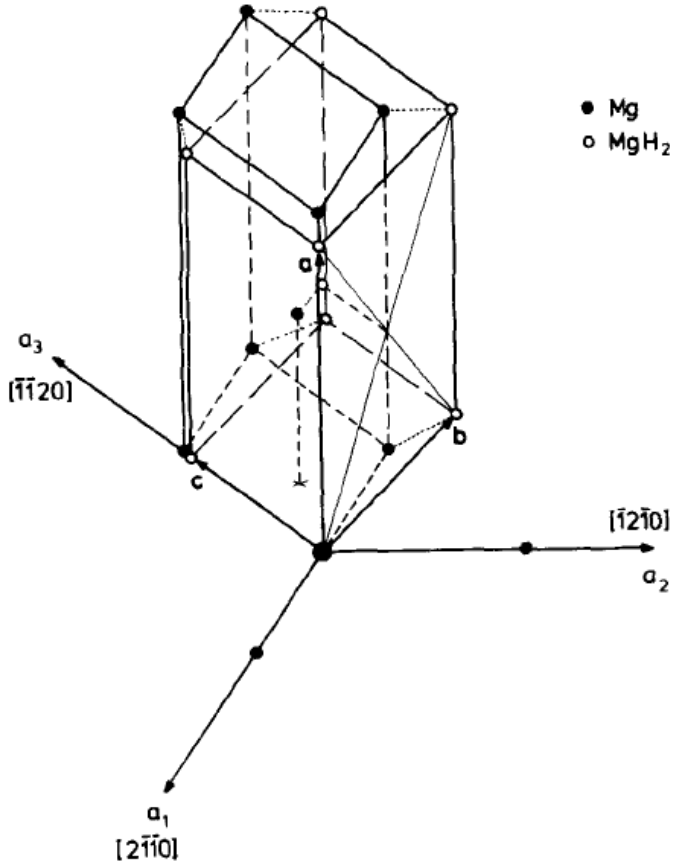

Figure 2.2 Graphical presentation of the Mg (001)[110] // MgH_2 (100)[001] orientation relationship between two unit cells of Mg and one unit cell of MgH_2 (only the metal atoms are shown). (Schöber, 1981)

Bokhonov *et al.* (1987) carried out a similar TEM study, in which they investigated the decomposition induced by an electron beam in MgH_2 single crystals and whiskers. In their study, the orientation relationship between MgH_2 and Mg lattices was found to be as Mg (001) // MgH_2 (110) (see Figure 2.3).

Kelekar *et al.* (2007) studied the hydride formation in epitaxial and textured magnesium thin films capped with palladium. They grew epitaxial Mg in the (001) orientation on Al_2O_3 (001) and in the (110) orientation on $LiGaO_2$ (320) as well as a textured Mg (001) on glass, and studied the formation of hydride at 373 K in 6 bar hydrogen gas by using x-ray diffraction techniques. As a result, it was shown that the hydride forms epitaxially relative to the Mg and the epitaxial relationship was given as Mg (001)[100] // MgH_2 (110)[001] on Al_2O_3 (as shown in Figure 2.4) and Mg (110)[111] // MgH_2 (200)[001] on $LiGaO_2$.

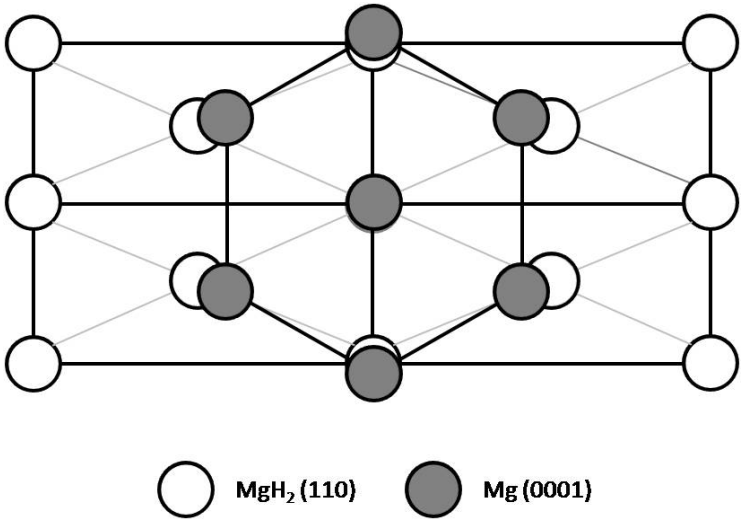

Figure 2.3 Graphical presentation of the Mg (001) // MgH_2 (110) orientation relationship along the phase boundary (only the Mg atoms are shown). (Bokhonov *et al.*, 1987)

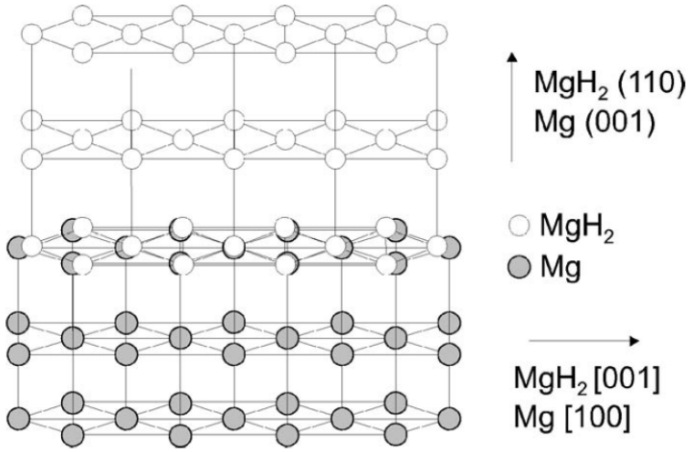

Figure 2.4 Schematic drawn to scale of the epitaxial growth mode of MgH_2 on Mg on (001) Al_2O_3 in the Mg (001)[100] // MgH_2 (110)[001] configuration. For clarity, only the Mg atoms in MgH_2 are shown. (Kelekar *et al.*, 2007)

Magnesium thin films, in the as-deposited state, could be crystalline with or without a texture or amorphous depending on the conditions of deposition. Singh *et al.* (2007) and Vermeulen *et al.* (2008) have sputter deposited films with a random texture, i.e. all reflections appeared in the x-ray diffraction pattern. Léon *et al.* (2002) and Akyıldız *et al.* (2006) using a thermal evaporation technique have obtained similar structures, i.e. films with a random texture. Upon hydrogenation of these films, normally carried out under isothermal conditions, Mg was converted into MgH_2 again with a random texture. In the majority of cases in the literature, however, thin films that have been deposited are strongly textured with (001) parallel to the substrate (Kumar *et al.*, 2008; Yamamoto *et al.*, 2002; Higuchi *et al.*, 2002). Hydrogenation, under such conditions, leads to formation of a textured MgH_2 with (110) parallel to the substrate.

Kelekar *et al.* (2007) pointed out that Mg on glass exhibited a single (001) out-of-plane orientation in the as-deposited state. Only (110) reflections of MgH_2 were seen after the hydrogen uptake, showing that the MgH_2 phase grows in a specific orientation relative to the Mg.

Recently, Singh *et al.* (2007) studied the structural and hydrogen storage properties of nanostructured Mg thin films deposited on Si (001) substrates. In their study, x-ray diffraction results revealed that the Mg to MgH_2 transformation follows a martensitic-like orientation relationship with Mg (002) // MgH_2 (110) and Mg [1-20] // MgH_2 [111], which was further confirmed by using selected area electron diffraction (SAED).

A similar relationship was also reported by Higuchi *et al.* (1999, 2002). In both of their studies, they emphasized that magnesium hydride formation in Mg thin films deposited on glass substrates follows a martensite-like transformation in which Mg (*00l*) relates with MgH_2 (*hh0*).

2.1.2 Thermodynamics of Hydrogen Uptake

Krozer and Kasemo (1989, 1990) and Rydén *et al.* (1989) concentrated on obtaining equilibrium data for thin film Mg–H system and therefore designating a region in the temperature-pressure plane where such data can be obtained.

After an extensive research, the limits of this region were demystified by Krozer and Kasemo (1990): the lower temperature limit is pressure-dependent and it is the maximum temperature at which an interface hydride forms, the upper temperature limit is the temperature at which intermixing/alloying between palladium and magnesium starts, and the pressures employed must be moderate since at too low pressures the uptake rate becomes so small resulting in

impractically long equilibration times and at too high pressures the uptake becomes so rapid that the dissipated chemical energy of the exothermic hydrogenation reaction raises the temperature of the sample and thus preventing measurements under isothermal conditions. By studying thermodynamics of hydrogen uptake within the specified limits, Krozer and Kasemo (1989, 1990) also determined the enthalpies of hydride formation and decomposition for magnesium thin films as 60.7 ± 6.3 kJ mol^{-1} H_2 and 71.2 ± 4.2 kJ mol^{-1} H_2, respectively. The Van't Hoff plot representing the hydrogenation properties of magnesium thin films is given in Figure 2.5.

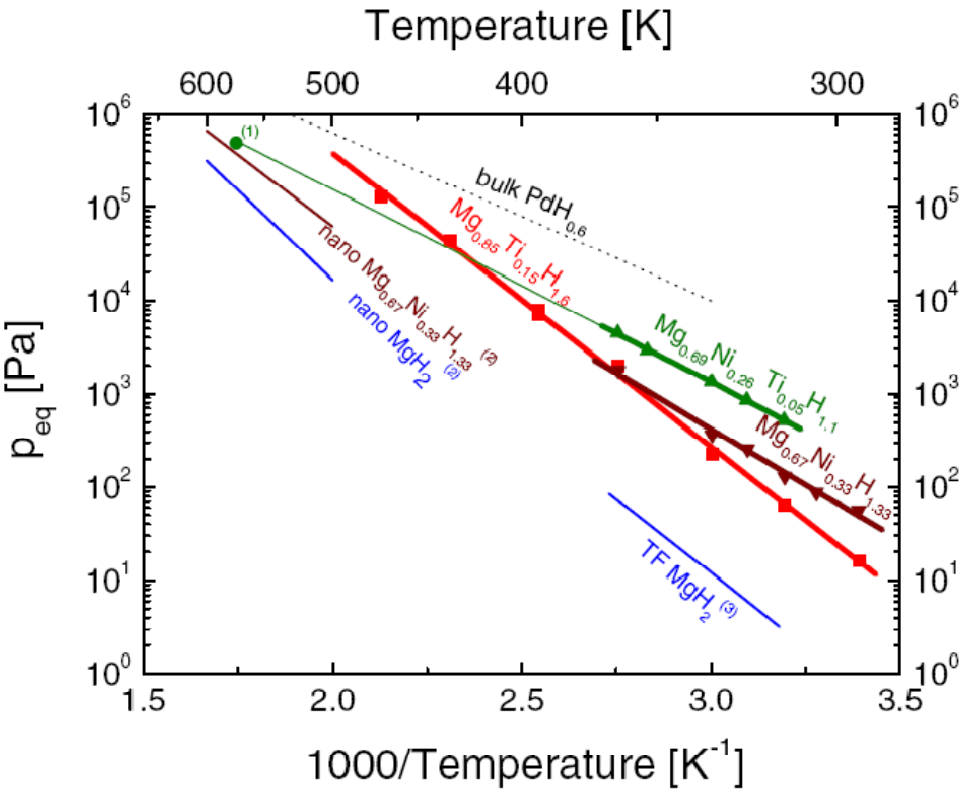

Figure 2.5 Van't Hoff plots for the hydrogenation of some Mg-based materials systems. The numbers between parentheses refer to: (1) Liang *et al.* (1999), (2) Liang *et al.* (1998) for nanocrystalline hydrides, and (3) Krozer and Kasemo (1989) for thin films (TF). (Dam *et al.*, 2007)

2.1.3 The Pressure Dependent Kinetics of Hydrogen Uptake

As already mentioned previously, the experimental results on the hydriding behavior of palladium-covered magnesium thin films were first reported by Krozer and Kasemo in 1987. Unusual kinetics was observed in their study: the hydrogen uptake saturated far from stoichiometric MgH_2 at room temperature and the saturation uptake decreased with increasing hydrogen pressure. This negative pressure dependency of hydrogenation was attributed to the formation of a thin hydride layer at the Pd/Mg interface that blocks further hydrogen uptake because of the slow hydrogen diffusion in the magnesium hydride.

In order to support this argument, Krozer and Kasemo (1987) designed a basic experiment in which they examined the hydriding characteristics of a Pd/Mg/Pd/Mg sandwich layer that has three Pd/Mg interfaces. Their idea was quite simple: if all the hydrogen were trapped in the form of interface hydride, then this structure would be expected to take up three times more hydrogen than the Pd/Mg structure, since it has three Pd/Mg interfaces whereas Pd/Mg structure has only one. The result of this experiment supported the interface hydride formation hypothesis: the uptake increased in the Pd/Mg/Pd/Mg structure by more than a factor of two, suggesting a hydrogen distribution where majority of hydrogen atoms are trapped at the Pd/Mg interface(s).

Although the formation of an interface hydride was inferred from the kinetic results obtained by Krozer and Kasemo (1987), the definitive proof was given two years later by Rydén *et al.* (1989). In their study, hydrogen depth profiling using a resonant nuclear reaction verified the existence of an interface hydride. The hydrogen depth profiling results obtained with the structures having multiple Pd/Mg interfaces also showed a strong increase in hydrogen

concentration at the interfaces, suggesting a thermodynamic driving force for the formation of this interface hydride.

Further experiments done by Rydén *et al.* (1989) revealed that the nucleation rate and the growth of the hydride is faster at higher pressures, which results in the formation of a thinner interface hydride, i.e. decreased hydrogen uptake. Contrastingly, hydrogenation at lower pressures resulted in a hydride region which is thicker and containing a larger amount of hydrogen.

The effect of temperature on this pressure dependent behavior was investigated by Krozer and Kasemo (1989) as well as Rydén *et al.* (1989). Both studies concluded that the formation of an interface hydride can be prevented by increasing the temperature. As temperature increases the interface hydride is less possible to form, however at temperatures above 400 K intermixing and/or alloying between palladium and magnesium becomes significant as reported by Krozer and Kasemo (1987). Although it was suggested that the interface hydride formation can be related to the formation of a Mg-Pd alloy, experiments done by Krozer and Kasemo (1987) eliminated that possibility.

In their following study, Krozer and Kasemo (1990) showed that the temperature required to prevent interface hydride formation is also pressure dependent: the higher the pressure is, the higher the temperature. They also emphasized that significant Pd-Mg intermixing and/or alloying does not occur below 380 K.

There are only few publications that discussed the mechanism of hydride formation and the resulting negative pressure dependency. Krozer and Kasemo (1987) suggested that the formation of an interface hydride might be linked to the high hydrogen concentration gradient perpendicular to the surface. It was argued that the diffusion speed of hydrogen atoms in palladium is very high,

whereas diffusion is slower at the Pd/Mg interface and in magnesium. At higher pressures the hydrogen concentration in palladium therefore becomes larger, inducing interface hydride formation at a smaller total hydrogen uptake, than at low pressures where the gradients become successively weaker. However, this argument was invalidated by Rydén *et al.* (1989) since it could not explain the appearance of high hydrogen concentrations at the internal Pd/Mg interfaces.

Krozer and Kasemo (1987) also stated that the mechanism of hydride formation can alternatively be discussed in terms of how the hydrogen heat of solution depends on local electron density. In their study, it was emphasized that the lattice mismatch at the Pd/Mg interface certainly creates defects with low atomic density/electron density, which gives an enrichment of hydrogen at the Pd/Mg interface(s) during hydriding. Nucleation occurs when the hydrogen concentration reaches a critical value, followed by hydride growth, predominantly along the interface. It was also stated that lowering in electron density due to the lattice expansion during hydriding possibly contributes to the growth and eventually a coherent interface hydride forms.

Rydén *et al.* (1989), on the other hand, pointed out three possible mechanisms of interface hydride formation: (i) trapping of hydrogen at defects on the surface or interface as already suggested by Krozer and Kasemo (1987), (ii) easier formation of hydride nuclei at the surface due to the lower energy requirement (in terms of lattice strain) of expansion during hydrogenation at the surface than in the bulk, and (iii) occurrence of Mg-Pd local alloying over a few atomic layers at the interface and thereby creation of hydride nuclei formation centers which subsequently grow to form the hydride layer. There, it was also emphasized that surface hydride formation seen to be more frequent than expected and it is not unlikely that the high temperatures required for hydriding of magnesium is at least partly caused by surface hydride formation. These studies also successfully

showed that an interface between two metals can induce nucleation and growth of an interface hydride.

2.1.4 Optical Switching Upon Hydrogen Sorption

Huiberts *et al.* (1996a) discovered that rare earth (RE) thin films coated with a thin layer of palladium exhibit a reversible metal-to-insulator transition accompanied by drastic changes in their optical properties when exposed to hydrogen gas. In the meantime, it was found by van der Sluis *et al.* (1997) that also the hydrides of rare earth-magnesium alloys show a similar behavior upon absorption of hydrogen. Differently from the RE hydrides, Mg-RE alloy thin films exhibited three different optical states: a color-neutral transparent state at high hydrogen concentrations, a non-transparent dark absorbing state at intermediate hydrogen pressures and a highly reflective metallic state at low hydrogen pressures, see Figure 2.6. In 2001, Richardson *et al.* reported switchable mirror effects in thin films of Mg and 3d transition metals (TM), which avoid the use of rare earth metals and may therefore be more cost-effective and stable. This development resulted in tremendous amount of research on Mg-TM alloys.

Since MgH_2 is a transparent, color-neutral insulator with a band gap of 5.6 eV as reported by Isidorsson *et al.* (2003), magnesium films capped with a thin layer of palladium is expected to become transparent upon exposure to hydrogen. However, van der Sluis *et al.* (1997) reported that pure Mg films could not be loaded with enough hydrogen to become transparent, presumably due to the slow diffusion of hydrogen in MgH_2. Several years later, Yamamoto *et al.* (2002) studied the hydrogenation behaviors of 200 nm thick Mg films with Pd overlayers at 373 K under 0.1 MPa (i.e. 1 bar) H_2 gas. At the end of 24 hours, Mg thin films changed from shiny mirror state into a color-neutral transparent state.

The first study, in which the optical properties of magnesium thin films were used to represent the hydrogen concentrations within the samples, was reported by Yoshimura *et al.* (2004). In their study, Yoshimura *et al.* (2004) investigated the hydrogenation properties of Pd-capped pure Mg thin films by monitoring the optical reflectance of the sample surface. Similarly, Qu *et al.* (2009) studied the hydrogen sorption properties of Pd-capped Mg thin films by monitoring the optical transmittances. Shalaan and Schmitt (2006) found that Mg nanoparticle films show improved absorption-desorption kinetics and switching properties in comparison to Mg polycrystalline films. By exposing these films to normal pressure of hydrogen gas at room temperature, they obtained transparent MgH_2 in less than 100 seconds.

Recently, Gremaud *et al.* (2007) proposed a new combinatorial method (i.e. hydrogenography) based on the fact that hydrogen absorption in a metal leads to large optical changes. They further showed that besides being a monitoring technique, "hydrogenography" also provides a high-throughput method to quantitatively measure the key thermodynamic properties such as enthalpy and entropy of hydride formation.

Figure 2.6 Transparent, dark and reflective states of a $Gd_{30}Mg_{70}$ alloy. The states can be switched by pumping hydrogen in and out of a cell that contains the alloy film. (Ball, 1998)

CHAPTER 3

EXPERIMENTAL DETAILS

3.1 Materials

Magnesium turnings (−4 mesh) from *Alfa Aesar* and a palladium rod (0.125″ diameter x 10 cm long) from *Kurt J. Lesker Co.* were used in the experiments. The purities of magnesium and palladium were 99.98 and 99.95%, respectively. Magnesium turnings were evaporated in their original form, whereas small chips were cut from the palladium rod. Hydrogen gas used in the experiments was typically 99.995% pure.

3.2 Deposition of Magnesium Thin Films

Pure and palladium-covered magnesium thin films were deposited on glass substrates by using a custom-made thermal evaporation unit (Akyıldız, 2009). This apparatus is made up of a stainless steel base plate (278 mm in diameter, 160 mm in depth) and a stainless steel bell jar with a height of 430 mm. The unit has four evaporation sources (Sorensen DCS8-350E, manual/automatic current (0-350 A) or voltage control (0-8 V)), which could be controlled independently with four rotational shutters.

Ultra high vacuum (UHV) conditions inside the unit are established by the cooperative action of dry mechanical (Adixen ACP15) and turbo-molecular (Adixen ATP150) pumps. A vacuum gauge (Adixen AHC2010) and its display unit (Adixen ACM2000) are also attached to the system in order to monitor the vacuum level during deposition. Photograph of this custom-made thermal evaporation unit is given in Figure 3.1.

Substrates were commercial grade soda lime glass with an approximate chemical composition of 72.20% SiO_2, 14.30% Na_2O, 6.40% CaO, 4.30% MgO, 1.20% Al_2O_3, 1.20% K_2O, 0.03% SO_3 and 0.03% Fe_2O_3. They were 0.17 mm thick, 24 mm in diameter. Prior to deposition, substrates were cleaned ultrasonically. The procedure was as follows: (i) ultrasonic cleaning in heated deionized water and detergent solution for an hour, (ii) rinsing under tap water for 5-10 minutes, (iii) ultrasonic rinsing in tap water for 15 minutes, (iv) rinsing with deionized water, (v) ultrasonic rinsing in deionized water for 15 minutes, (vi) rinsing with ethanol, and (vii) ultrasonic cleaning in ethanol bath for 15 minutes. The substrates were then dried by a hot-air dryer and subsequently placed on the substrate holder inside the thermal evaporation unit.

An alumina (Al_2O_3) crucible within a tungsten basket heater was used as the evaporation source for magnesium turnings. Palladium, on the other hand, was evaporated in the form of chips by using a tungsten boat. Schematic representation of the deposition chamber indicating the relative positions of these evaporation sources is given in Figure 3.2. Before deposition, the whole system was baked-out by the use of an infrared quartz heater in order to degas and remove impurities which are adsorbed/absorbed by the evaporation materials. The system was then cooled down to room temperature and deposition was initiated. Substrate temperature recorded as a function of time during the deposition of Pd-covered Mg thin films is shown in Figure 3.3.

Figure 3.1 The custom-made thermal evaporation unit. (Akyıldız, 2009)

All thin films in this study were produced under UHV conditions with a base pressure of 1×10^{-7} mbar. Source to substrate distance was typically 350 mm. The deposition rate during evaporation was monitored by using a quartz crystal thickness monitor (SQC-310 Deposition Controller, Sigma Instruments). Typical deposition rate of magnesium was 1 nm/s. A thin layer of palladium was subsequently deposited on magnesium by flash evaporation. The thickness of the underlying Mg layer was typically 350 nm, where present Pd overlayer thickness ranged from 6 to 48 nm.

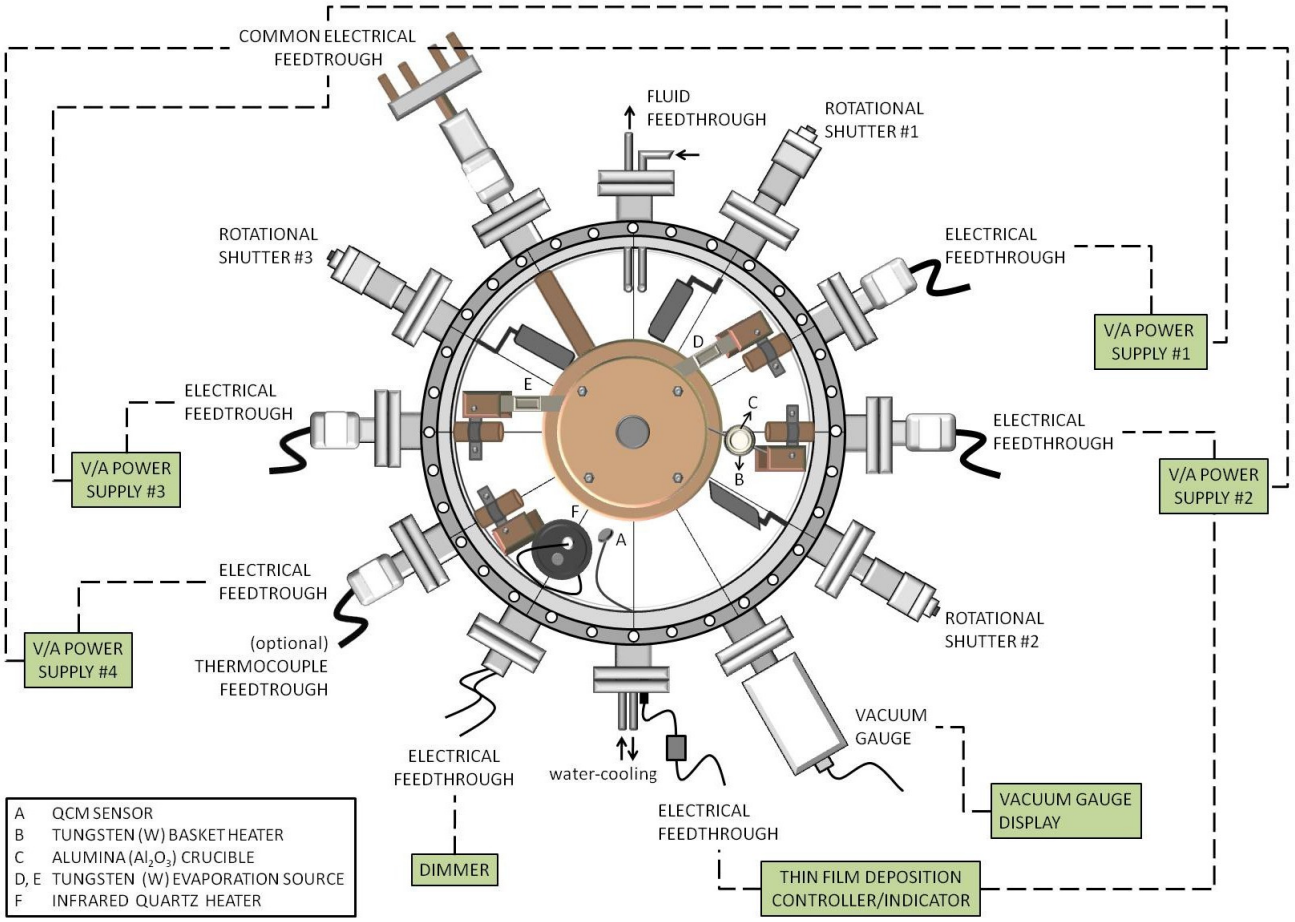

Figure 3.2 Schematic representation of the deposition chamber constructed by Akyıldız (2009).

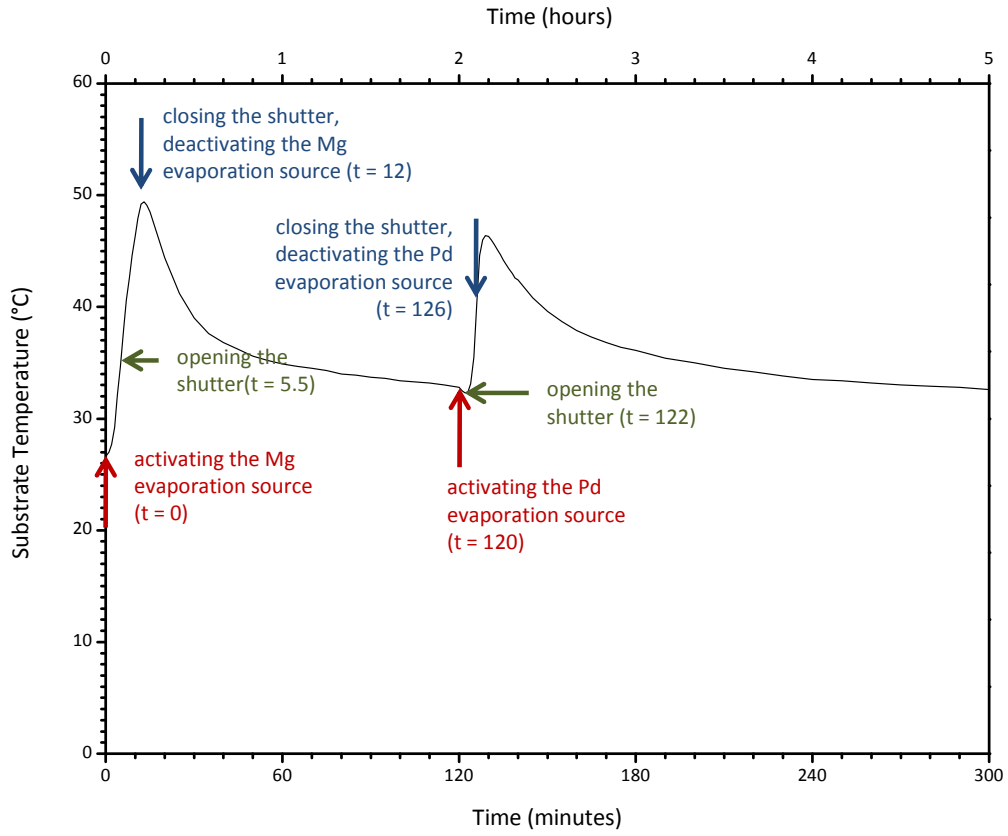

Figure 3.3 Variation in substrate temperature during the deposition of Pd-covered Mg thin films via thermal evaporation.

3.3 Hydrogenation of Magnesium Thin Films

A set-up was constructed for measuring the hydrogen sorption properties of magnesium thin films by means of resistance measurements. During the design stage of this resistance measurement set-up (RMS), following requirements were taken into account: (i) the set-up must stand an internal gas pressure of at least 10 bar at the temperatures ranging from room temperature to 473 K, (ii) it must be leak-tight down to the lowest testable level both under vacuum conditions (10^{-4} mbar) and for pressures up to 10 bar, and must remain so for the temperatures

up to 473 K, and (iii) the volume inside the set-up must be as small as possible. The schematic representation of this set-up is given in Figure 3.4.

The body of the set-up consists of four main parts, where the numbering refers to Figure 3.4. Unless stated otherwise, all parts of the set-up were made up of 316 stainless steel. The essential part of this set-up is the main chamber (1) which houses the sample stage and the gas feed-through. The gas feed-through is closeable by a miniature ball valve and therefore the whole set-up, if needed, can be disconnected from the gas supply.

The second part is the probe-holder (2), which was produced by molding two spring loaded gold-plated probes (INGUN Test Probes, GKS-100-201-90-A) in cold-setting embedding resin within a custom-made stainless steel die that is capable of molding up to four probes. The general view and dimensional details of this die are given in Figure 3.5 and Figure 3.6, respectively. Prior to molding process, a thin layer of wax was applied on the inner surfaces of the die in order to ensure a safe removal. In the as-produced probe-holder, a probe spacing of 12 mm was obtained. As the final steps, tips of the probes were rounded by mounting tiny drops of gold (approximately 2 mm in diameter) and electrical connections were established by soldering copper cables to the back sides of the probes. The following part of this set-up is the "connector" (3), only function of it being connecting the probe-holder to the main chamber. Last major component is the lid (4), which is in fact a slightly modified standard 2¾ inch CF flange. Dimensional details of the lid, main chamber and connector are given in Figure 3.7.

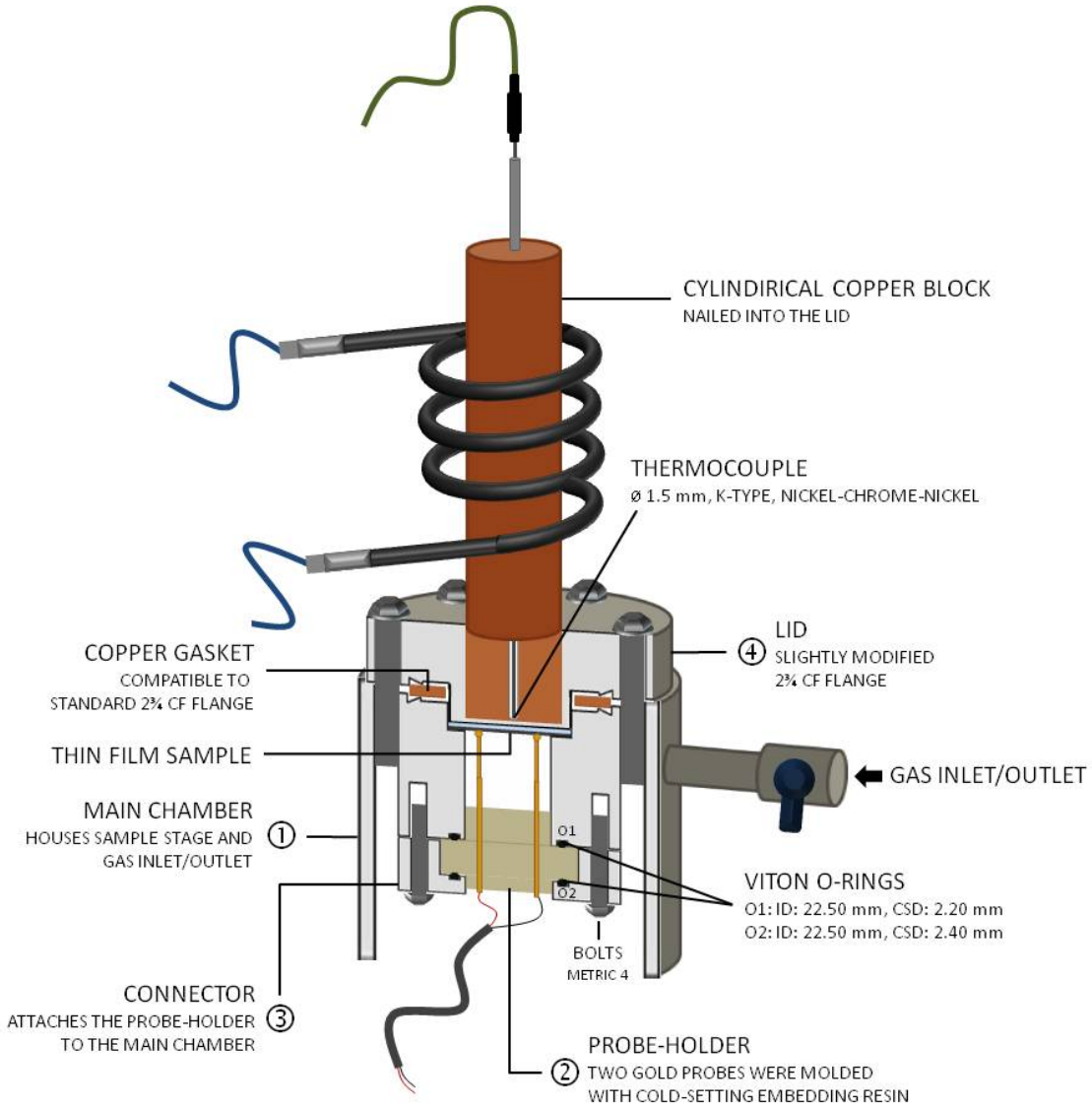

Figure 3.4 Cross-sectional schematic of the custom-made resistance measurement set-up.

In order to assure leak-tight seals in the pressure range from 10^{-4} mbar to 10 bar and temperature range from room temperature to 473 K, two viton o-rings (inner diameter of 22.50 mm, cross-sectional diameter of 2.20 or 2.40 mm) were placed into the o-ring grooves existent on the lower and upper surfaces of the main chamber and the connector, respectively. The probe-holder was then inserted into the main chamber and the connector (3) was placed against its lower surface. The main chamber and the connector were then tightly fixed together by the use of six bolts (metric 4 x 20 mm). Whenever a thin film sample was inserted on the sample stage, the set-up was closed by tightly bolting the lid and the main chamber together, with a copper gasket in between, by again using six bolts (metric 6 x 20 mm).

Dimensions of the lid ensured full contact between the gold probes and the film surface. Resistance of the thin film sample was therefore easily measured at desired temperatures and hydrogen pressures by the use of a multimeter.

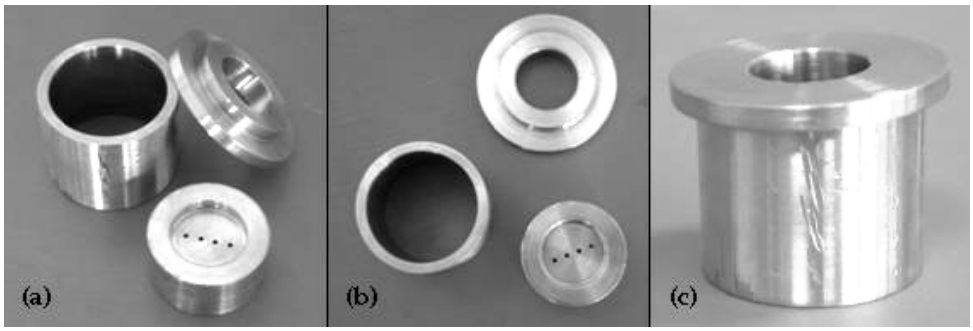

Figure 3.5 General view of the custom-made die used for the production of probe-holder.

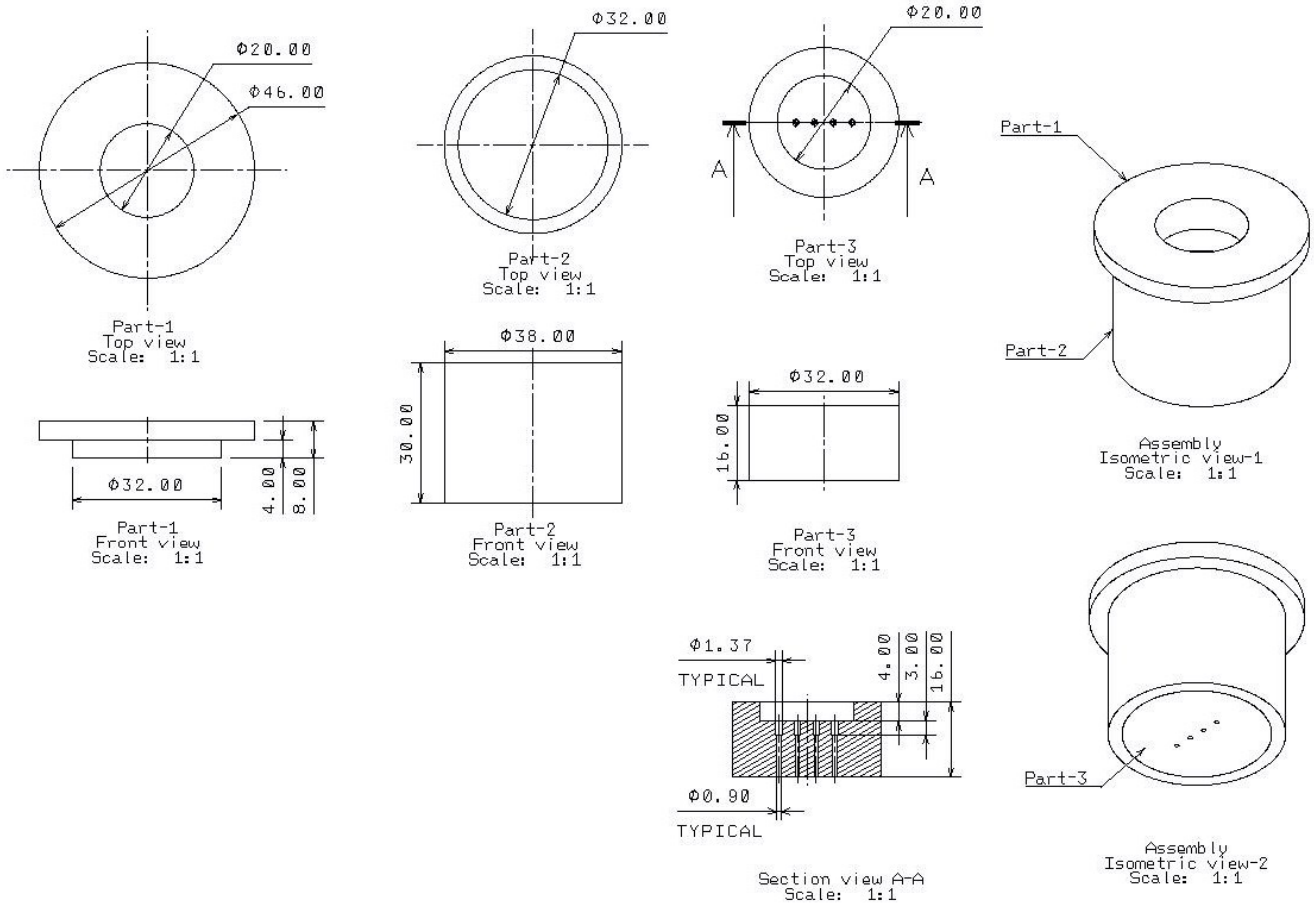

Figure 3.6 Dimensional details of the custom-designed die, which was used for the production of probe-holder.

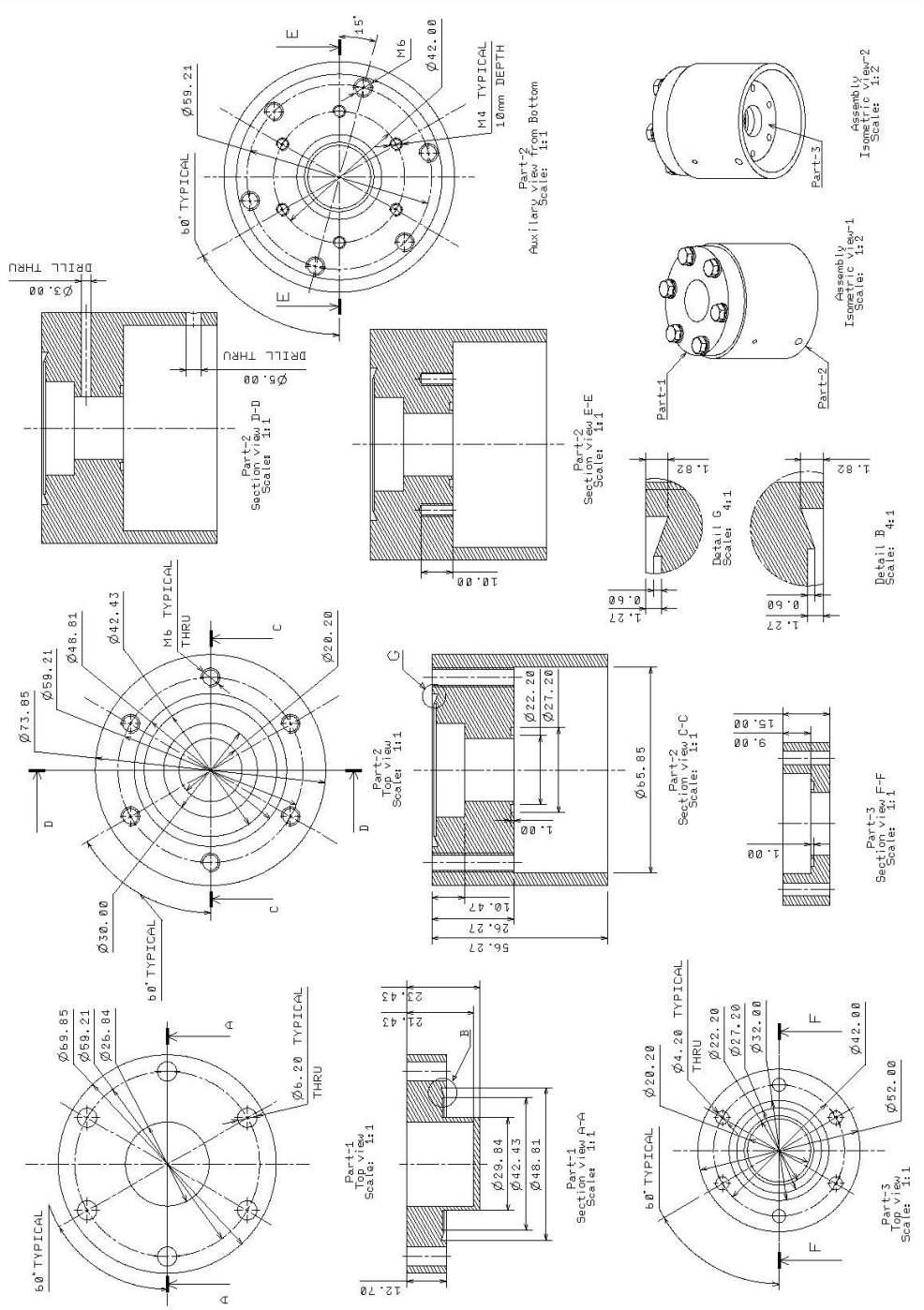

Figure 3.7 Dimensional details of the lid, main chamber and the connector.

During the experiments, temperature of the sample was controlled through a cylindrical copper block (27 mm diameter x 200 mm height) that was permanently nailed into the cylindrical cavity existing on the upper surface of the lid (see Figure 3.4 on page 27). Heating was accomplished by the use of a resistive coil, which was connected to a solid state relay (GEMO, 25A) and then attached to the temperature controller (Tetcis PC771).

In order to prevent temperature fluctuations at relatively high temperatures, a thermocouple (named as the "controller thermocouple") was placed close to the resistive heater coil and attached to a temperature controller. The actual temperature of the sample was then monitored by the use of a K-type nickel-chrome-nickel thermocouple that was inserted into the thermocouple receptacle existing inside the nailed copper block.

In order to access to the turbo-molecular pump system (Leybold AG PT 50) as well as to high purity argon and hydrogen gas sources, resistance measurement unit was connected to the main hydrogen sorption measurement set-up, which had originally developed by Baybörü (2001) and then improved by Güvendiren (2003), and was not disconnected unless it is mandatory. The photograph and the schematic layout of the main hydrogen sorption measurement set-up together with the resistance measurement unit are given in Figure 3.8 and Figure 3.9, respectively.

A piezoresistive pressure transmitter (KELLER PAA-23) and a relief valve were also connected near to the resistance measurement set-up (RMS) in order to perform experiments within the desired pressure limits, as well as monitoring the pressure inside the RMS.

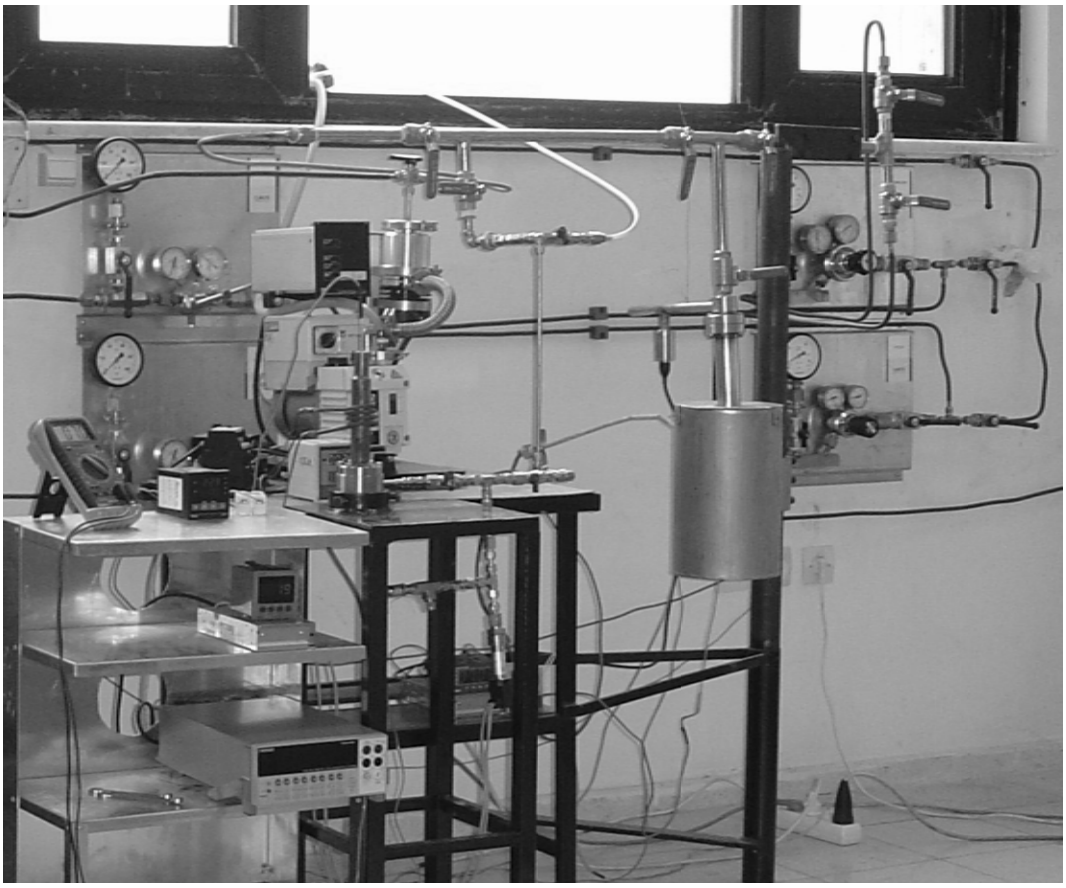

Figure 3.8 General view of the main hydrogen sorption measurement set-up together with the resistance measurement unit.

3.3.1 Isothermal Hydrogenation

Pd-covered Mg thin film sample was inserted onto the sample stage inside the resistance measurement set-up (RMS) and the set-up was then closed. The whole system was evacuated by opening vacuum (V), control (C_1, C_2, C_3, and C_4) and pressure transmitter (P) valves and flushed with argon gas (see Figure 3.9). Flushing was accomplished by closing the vacuum valve (V) and then introducing argon gas (99.998% pure, $P_{Ar} \approx 1$ bar) into the system by opening the argon valve (A). The system was then again evacuated by closing the argon valve

(A) and opening the vacuum valve (V). This procedure was repeated for three times in order to completely remove air within the RMS. The system was then slowly heated to the desired temperature in the evacuated state. Experiments were not initiated until the temperature of the sample was stabilized.

Vacuum (V) and control (C_1) valves were closed and the hydrogen gas of desired pressure was introduced into the system by opening the hydrogen valve (H). Immediately afterwards, the sample was exposed to hydrogen gas by opening the control valve (C_1). The pressure within the RMS was kept constant for 10 minutes. After 10 minutes, resistance of the sample was recorded and the pressure was adjusted to its next value. This procedure was repeated up to 1000 or 1500 mbar (i.e. 1 or 1.5 bar) with 20 mbar intervals. At the end of the experiment, thin film sample was cooled down to room temperature under the maximum hydrogen pressure applied.

3.3.2 Isochronal Hydrogenation

The sample was inserted onto the stage inside the RMS and the set-up was closed. After flushing with argon gas for three times, the system was evacuated for an hour. Vacuum (V) and control (C_1) valves were then closed and the hydrogen gas of desired pressure (i.e. 0.1, 0.5, 1 or 10 bar) was introduced into the system by opening the hydrogen valve (H). After the desired pressure was maintained within the system, the sample was exposed to hydrogen gas by simply opening the control valve (C_1). The pressure within the RMS was kept constant during the experiment.

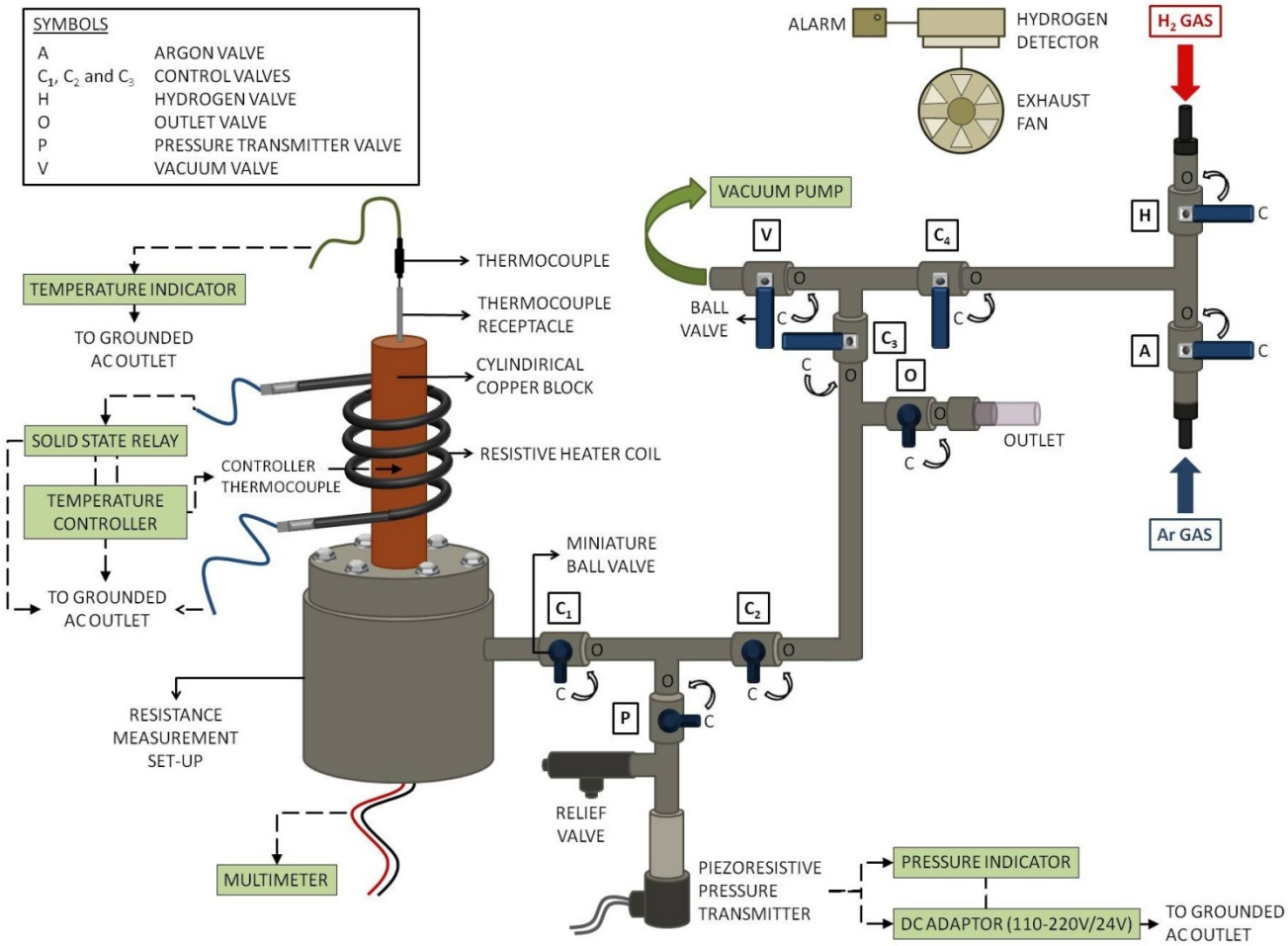

Figure 3.9 Schematic layout of the main hydrogen sorption measurement set-up together with the resistance measurement unit.

The system was then slowly heated - with a rate of 25 K/hour - up to 453 K at constant hydrogen pressure and the electrical resistance change was monitored. Higher temperatures were avoided in order to maintain the integrity of the resistance measurement set-up. At the end of six hours (i.e. at 453 K) experiment was terminated and the sample was cooled down to room temperature under the same (constant) hydrogen pressure.

3.4 Characterization of Magnesium Thin Films

X-ray diffraction measurements using Cu Kα radiation (λ = 1.54056 Å) were performed in ULTIMA^{+} D/MAX2200/PC Rigaku Diffractometer with Bragg-Brentano para-focusing beam configuration. Scan rate and sampling width were 1°/min and 0.02°, respectively.

Where needed, elemental analyses of the Pd-covered Mg thin films were accomplished by the use of an energy dispersive system (NORAN System 6 X-Ray Microanalysis System) that is attached to a Jeol JSM-6400 Scanning Microscope. For the structural characterization a FEI Quanta 400 Field Emission Scanning Electron Microscope (FESEM) was used.

Optical transmittances of the thin films at wavelengths from 300 to 1100 nm were measured from film sides by the use of UV1900 UV-VIS spectrophotometer with a scan interval of 0.5 nm.

CHAPTER 4

RESULTS AND DISCUSSION

The chapter starts with the as-deposited characterization of pure and palladium-covered magnesium thin films. Following this, a comparative study will be presented, in which the data obtained from two-point probe electrical resistance and optical transmittance measurement techniques will be questioned in terms of how well they represent the amount of MgH_2 formed in the samples. Finally, experimental results on the isothermal and isochronal hydrogenation behaviors of magnesium thin films will be reported, compared and discussed in detail.

4.1 As-Deposited Magnesium Thin Films

X-ray diffraction (XRD) profiles of 350 nm thick as-deposited Mg and Pd-covered Mg thin films are given in Figure 4.1 and Figure 4.2, respectively. It is seen that the patterns in both films contain only (002) and (004) reflections implying that the films have grown along the c-axes, i.e. (001) // glass substrate. The strongest peak is (002) reflection of the hexagonal close-packed (h.c.p.) Mg. X-ray diffraction pattern of pure magnesium powder, in which all the possible reflection planes of Mg are seen, is also given for comparison in Figure 4.3. Where present, Pd overlayer appears with all reflections; (111), (200) and (220), implying that Pd has formed and grown in a variety of orientations. Reflections

that belong to Pd start to appear as the overlayer thickness increases from 6 to 21 nm and become more intense with a further increase in thickness.

Figure 4.4 refers to a Mg thin film with 21 nm Pd overlayer, shows a typical image of the as-deposited thin film surface that displays a faceted structure. Surface elemental mapping of an as-deposited Mg/11 nm Pd thin film is given in Figure 4.5, showing that the Pd overlayer is homogenously deposited over the underlying Mg.

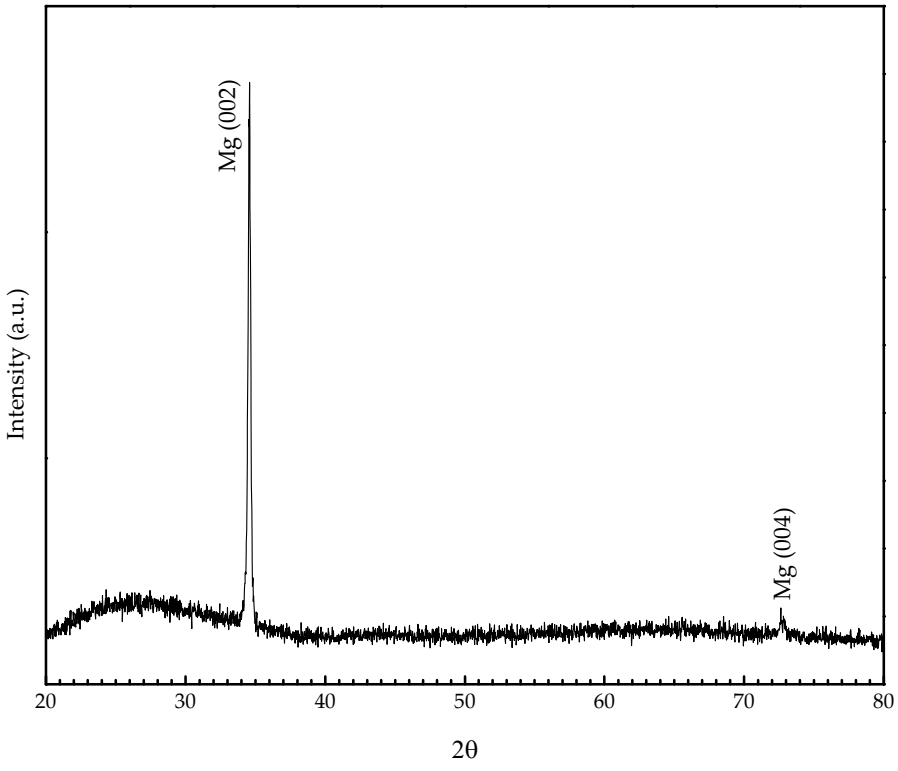

Figure 4.1 X-ray diffraction profile of an as-deposited 350 nm thick pure Mg thin film.

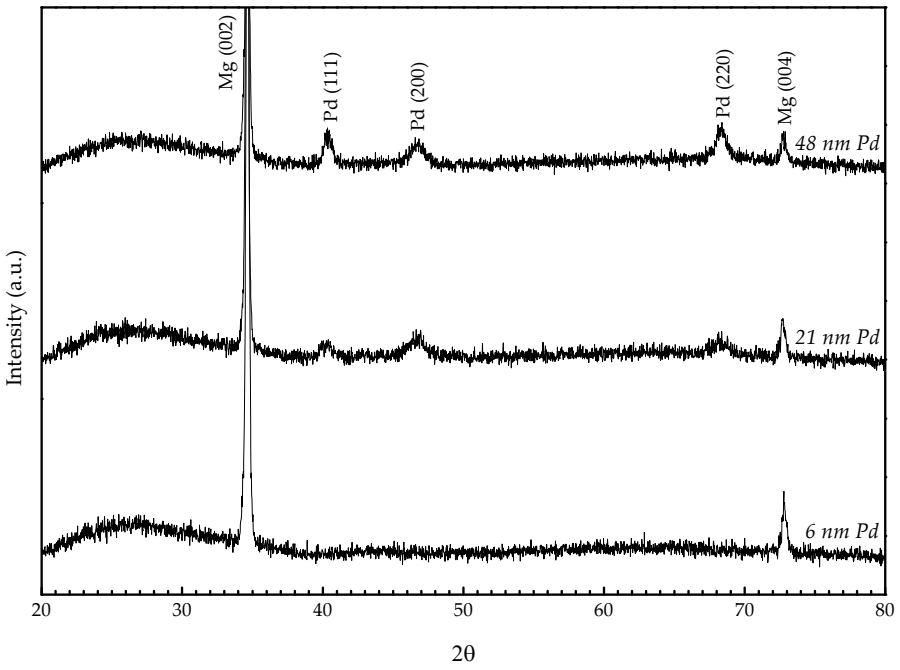

Figure 4.2 X-ray diffraction profiles of as-deposited 350 nm Mg/Pd thin films.

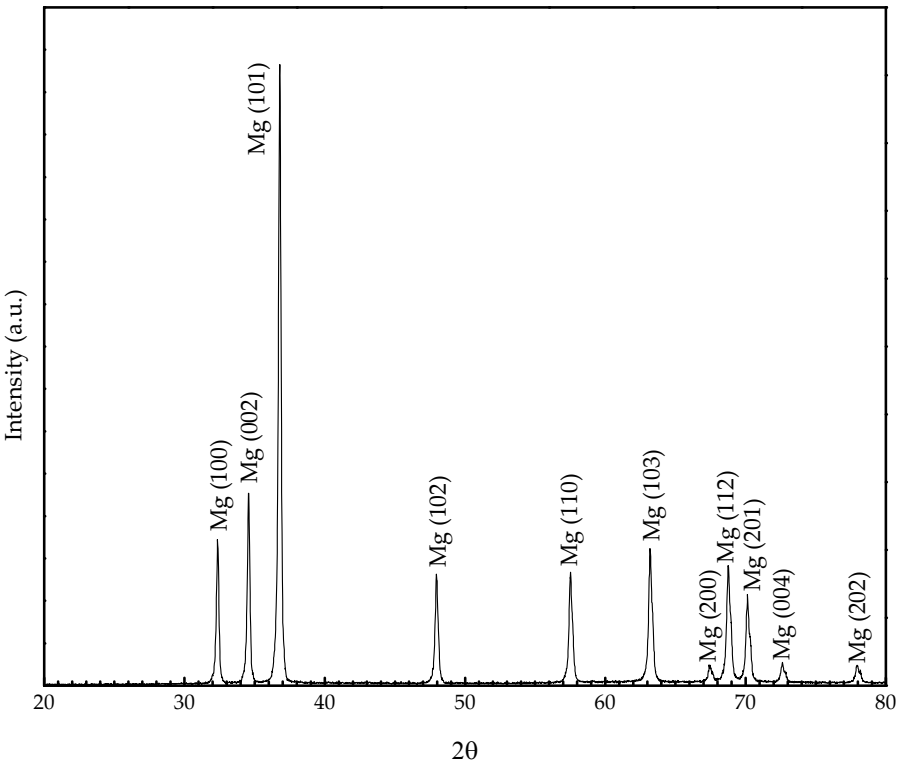

Figure 4.3 X-ray diffraction profile of pure magnesium powder.

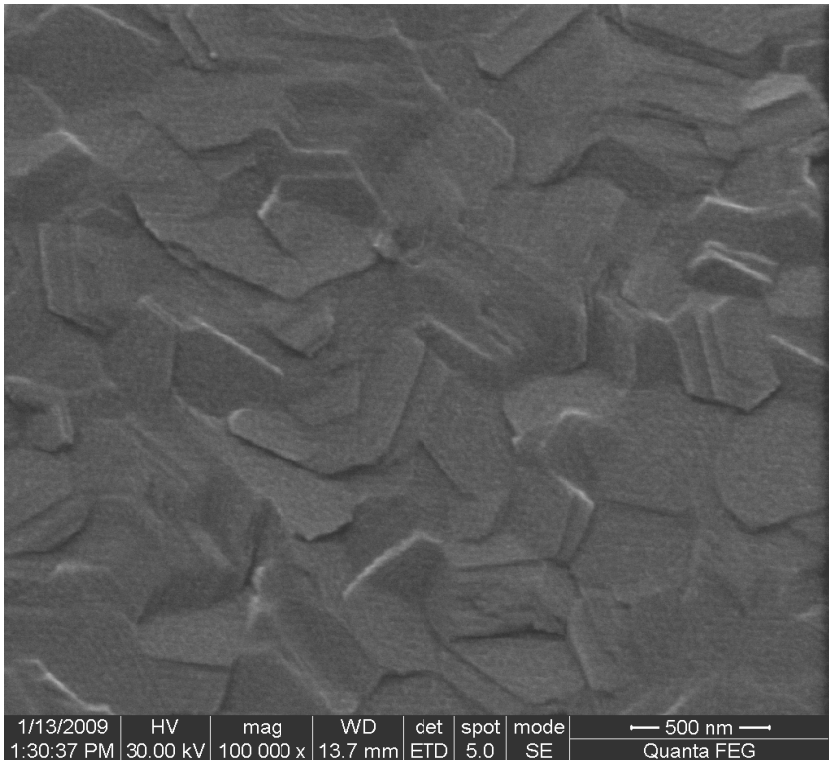

Figure 4.4 SEM surface image of an as-deposited 350 nm Mg/21 nm Pd thin film.

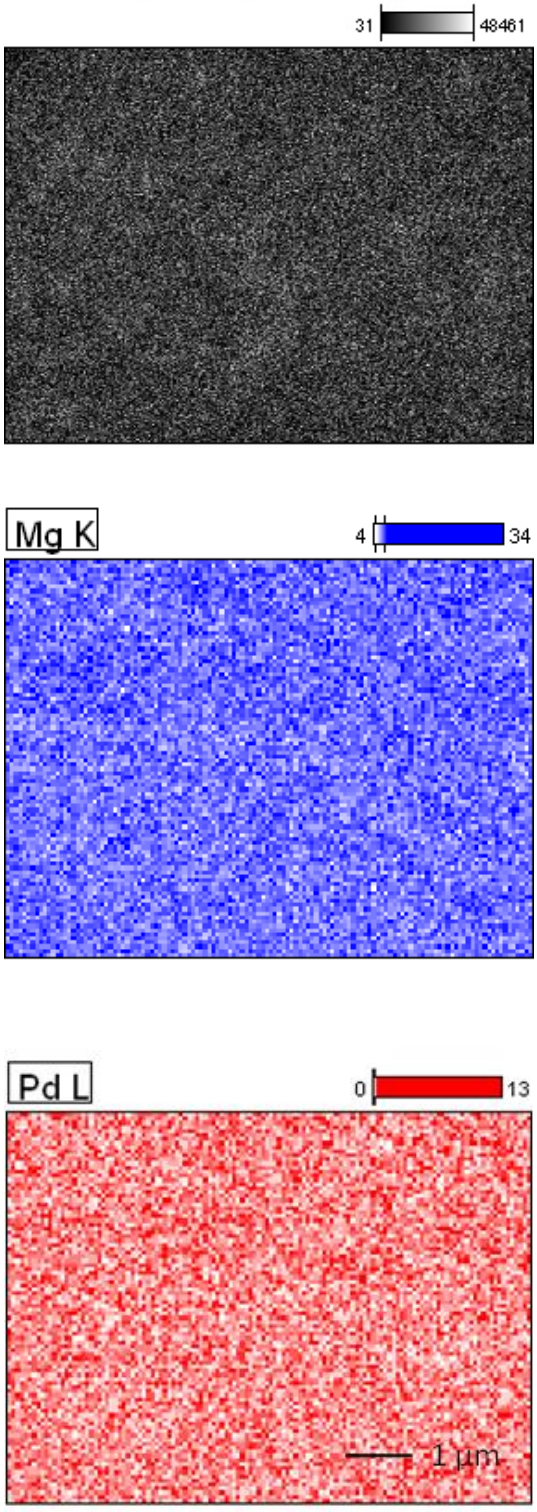

Figure 4.5 Surface elemental mapping (obtained at x15,000 magnification) of a Mg/11 nm Pd thin film. The blue and red colors correspond to Mg and Pd elements, respectively.

4.2 Hydrogen Absorption in Palladium-Covered Magnesium Thin Films Followed by Electrical Resistance and Optical Transmittance Measurements

In the context of this study, the amounts of MgH_2 formed within the samples were estimated by using the data obtained from electrical resistance and optical transmittance measurements, as well as x-ray diffraction studies. The procedure followed in the current study will be explained through a specific sample; 350 nm thick Mg thin film with a 10 nm Pd overlayer, hydrogenated isothermally at 363 K and 1 bar H_2 pressure for 6 hours.

A typical resistance vs. time plot obtained for this thin film sample is given in Figure 4.6. Following an incubation period, thin film sample shows a gradual increase in its resistance, implying that a considerable amount of Mg was transformed into MgH_2. Since any increase in resistance upon hydrogenation is directly related to the amount of hydride phase formed, relative hydrogen concentrations were estimated for Pd-covered Mg thin films by using their initial (R_i) and final (R_f) resistance values. In order to eliminate the anomalies arising from the differences in initial resistance values, data was represented in the form of percent resistance change with respect to initial resistance, i.e. $(R_f-R_i) / R_i * 100$.

It is also worth to mention that for the samples having a thicker Pd overlayer, same hydrogenation behavior was observed with a decreased resistance change. This is probably due to the negative contribution of Pd layer to overall resistance of the film, as it is known that Pd is always metallic irrespective of its hydrogen concentration (Huiberts *et al.*, 1996b). Since it is very difficult to correct this effect, only the samples having the same Pd overlayer thickness were evaluated with respect to each other. This was accomplished by expressing the largest value in each set as 100%.

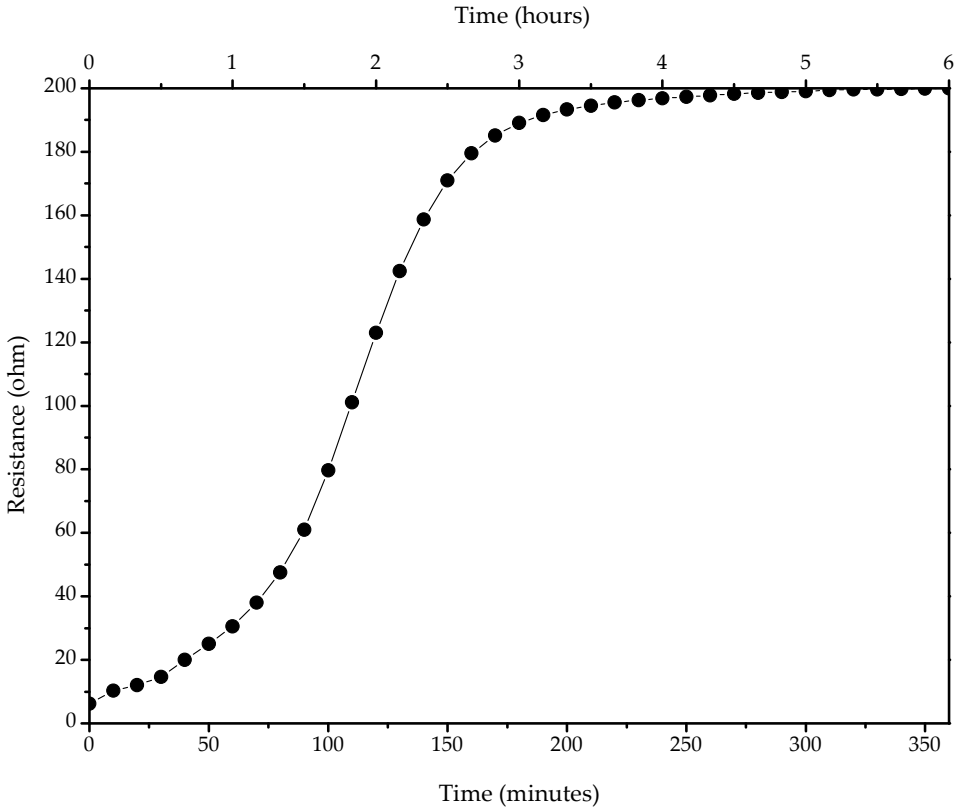

Figure 4.6 Relative resistance vs. time plot for 350 nm Mg/10 nm Pd thin film hydrogenated (1 bar) isothermally at 363 K.

Typical optical transmittance spectra obtained in as-deposited and hydrogenated states are both given in Figure 4.7. The amount of MgH_2 formed in a thin film sample was calculated from its transmission spectra by averaging the percent transmittance within the visible spectrum, i.e. 400-700 nm. Since transmittance data were not corrected for the effect of Pd overlayer, they were given for a constant Pd thickness.

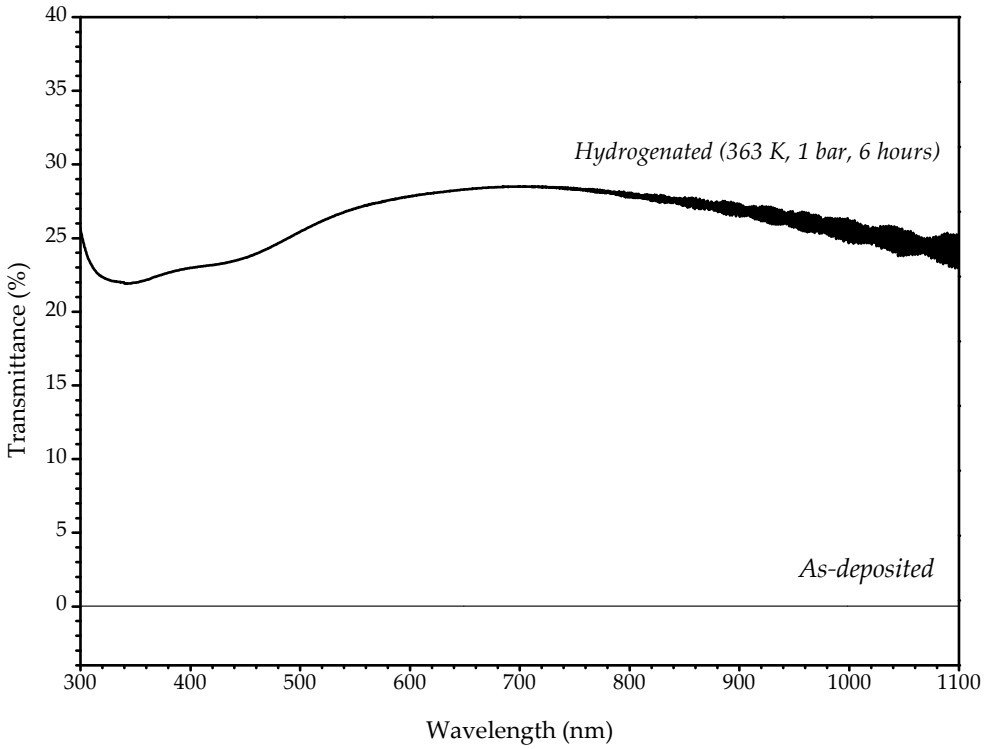

Figure 4.7 Optical transmittance spectra obtained for as-deposited and hydrogenated states of a 350 nm Mg/15 nm Pd thin film. Hydrogen loading was carried out isothermally.

X-ray diffraction profiles of the same sample in as-deposited and hydrogenated states are given in Figure 4.8(a) and (b), respectively. It is seen that Mg peaks coming from the basal plane has weakened considerably and instead MgH_2 peaks have developed upon hydrogenation. In the hydrogenated state, (110), (101), (200) and (211) peaks of the MgH_2 were observed.

Volume fractions of MgH_2 formed within the thin film samples were calculated from their x-ray diffraction profiles by applying the well-known quantitative phase analysis (QPA). The basis of this analysis is that the integrated intensity of reflections for a phase in a multiphase XRD pattern is related to the abundance of

that phase in the sample. Relying on this, (002) reflection of Mg with (110) and (101) reflections of MgH_2 are considered for the existing multiphase samples.

Throughout this study, 350 nm thick Mg thin films capped with 6, 10, 14, 15, 21 or 48 nm Pd were loaded with hydrogen at temperatures ranging from 298 to 453 K and pressures from 0.1 to 10 bar in a custom-made resistance measurement set-up. Hydrogenation behaviors of the samples were followed by in situ measurement of the film resistance. Optical transmittance spectrum and x-ray diffraction pattern were also obtained for the hydrogenated sample in question.

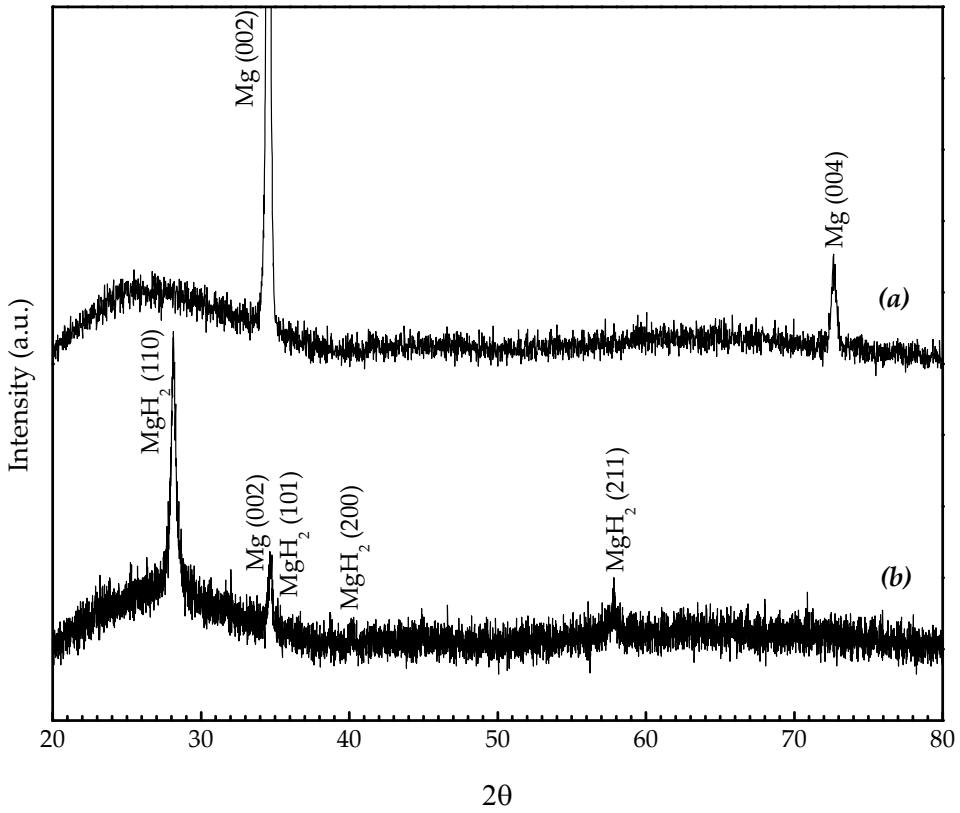

Figure 4.8 X-ray diffraction patterns of 350 nm Mg/10 nm Pd thin film; (a) in as-deposited state, (b) after isothermal hydrogenation (1 bar) at 363 K.

Results obtained from two-point probe electrical resistance and optical transmittance measurements were then both plotted as a function of x-ray diffraction (XRD) quantitative phase analysis (QPA) results for samples having the same palladium overlayer thickness, as shown in Figure 4.9. The data were then fitted linearly with an intercept at zero. Table 4.1 summarizes the R-squared values of these linear regressions, showing the strengths of the trends. As the R-squared value increases, the linear trend strengthens. To rephrase, the higher the R-squared value, the more closely "% resistance change" or "% transmittance" move in a linear relationship with the fraction transformed that was given in terms of volume %.

Figure 4.9 shows that data obtained from both measurement techniques behave linearly with those obtained from XRD QPA. However, for all the Pd thicknesses studied here, results of resistance measurements show larger scattering from the linear regression with respect to data obtained via optical transmittance measurements. In the case of optical transmittance measurements, the effect of Pd overlayer is clearly seen, i.e. the slope of the fit increases with an increase in Pd overlayer thickness.

The data obtained from both electrical resistance and optical transmittance measurements showed that best fit belongs to the sample with a 14 nm thick Pd overlayer. Moreover, resistance data obtained from Mg thin films showed good fits, i.e. above 90%, for all Pd overlayer thicknesses studied here. Good fits, above 85%, were obtained for samples having 6 to 14 nm Pd overlayers for both types of measurement technique. Also note that fits obtained for resistance measurements are superior in all cases (see Table 4.1), implying that the effect of palladium overlayer on transmittance of magnesium thin films is much pronounced than that on resistance. The worst fit, i.e. -0.809, was seen for the transmittance data of the sample having a 15 nm Pd overlayer.

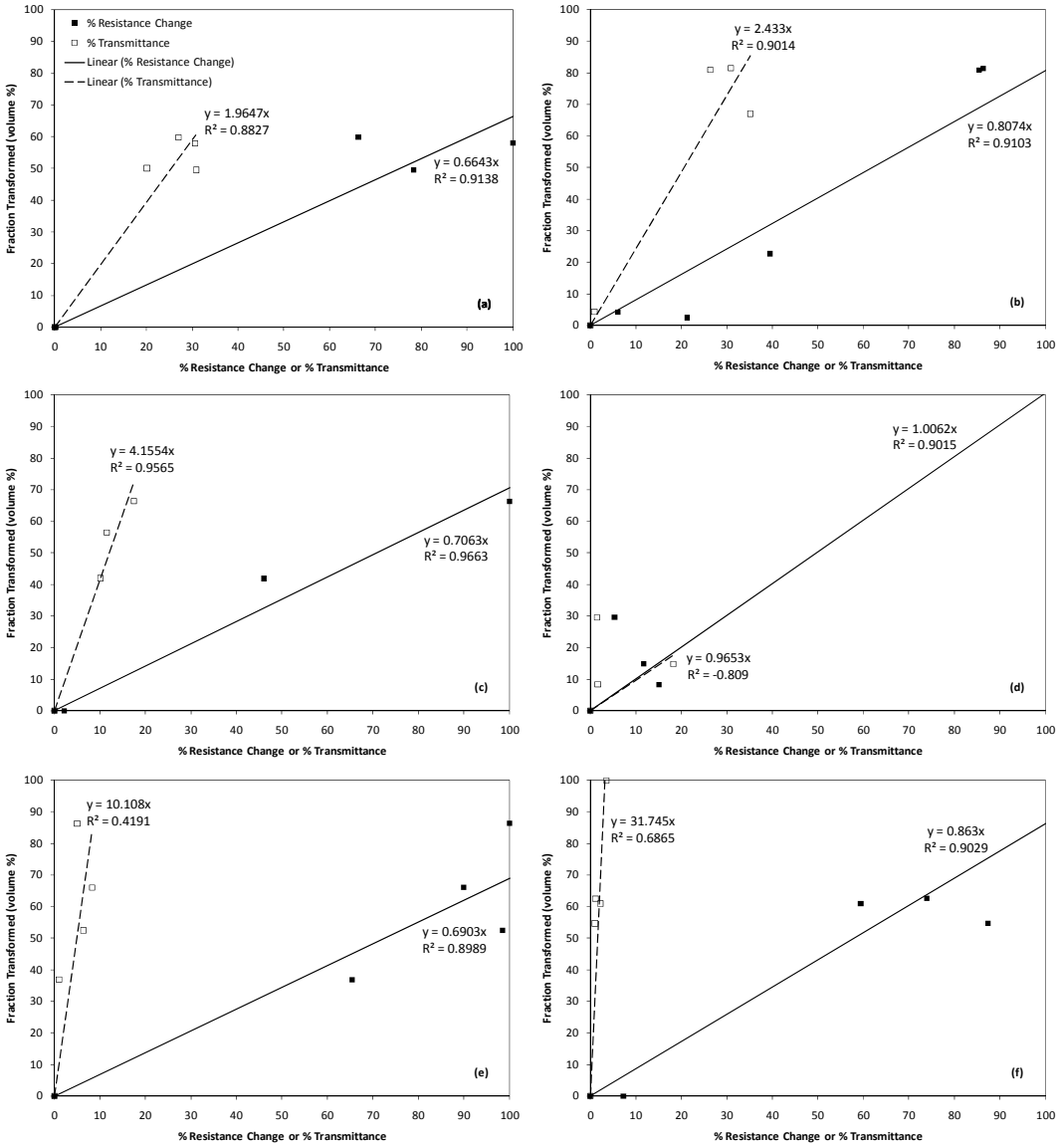

Figure 4.9 Data points and linear fits for the amount of MgH_2 formed in the samples, measured via two-point probe resistance and optical transmittance techniques in comparison with the XRD QPA results for 350 nm thick Mg thin films covered with (a) 6, (b) 10, (c) 14, (d) 15, (e) 21 and (f) 48 nm Pd.

Table 4.1 R-squared values of the linear regressions given in Figure 4.9.

Pd Overlayer Thickness (nm)	*R-Squared Values*	
	% Resistance Change	*% Transmittance*
6	*0.9138*	*0.8827*
10	*0.9103*	*0.9014*
14	*0.9663*	*0.9565*
15	*0.9015*	*-0.809*
21	*0.8989*	*0.4191*
48	*0.9029*	*0.6865*

Therefore, it seems like both two-point probe electrical resistance and optical transmittance measurements can be used to estimate the amount of MgH_2 formed in palladium-covered magnesium thin films. However, the effect of Pd overlayer is inevitable, especially in the case of optical transmittance measurements. These results suggest that fast and reliable experimentation with Mg thin film samples on their hydrogen sorption kinetics as well as thermodynamics are possible with one of these measurement techniques.

4.3 Hydrogenation of Magnesium Thin Films

350 nm thick magnesium thin films were hydrogenated in two different conditions; namely isothermal and isochronal. In the following sections, experimental results associated with the hydrogenation behavior of these films will be given and discussed in detail.

4.3.1 Isothermal Hydrogenation of Magnesium Thin Films

Pressure vs. relative resistance curves for isothermal hydrogenation of Pd-covered Mg thin films at 313, 333, 353 and 373 K are given in Figure 4.10. Here, the x-axis (namely relative resistance) was constructed by normalizing the values with respect to the highest resistance data observed in all four hydrogen loading experiments. It should be noted that, all experiments were performed under a maximum hydrogen pressure of 1 bar; except for the one that conducted at 373 K, in which the hydrogenation was carried on up to 1.5 bar.

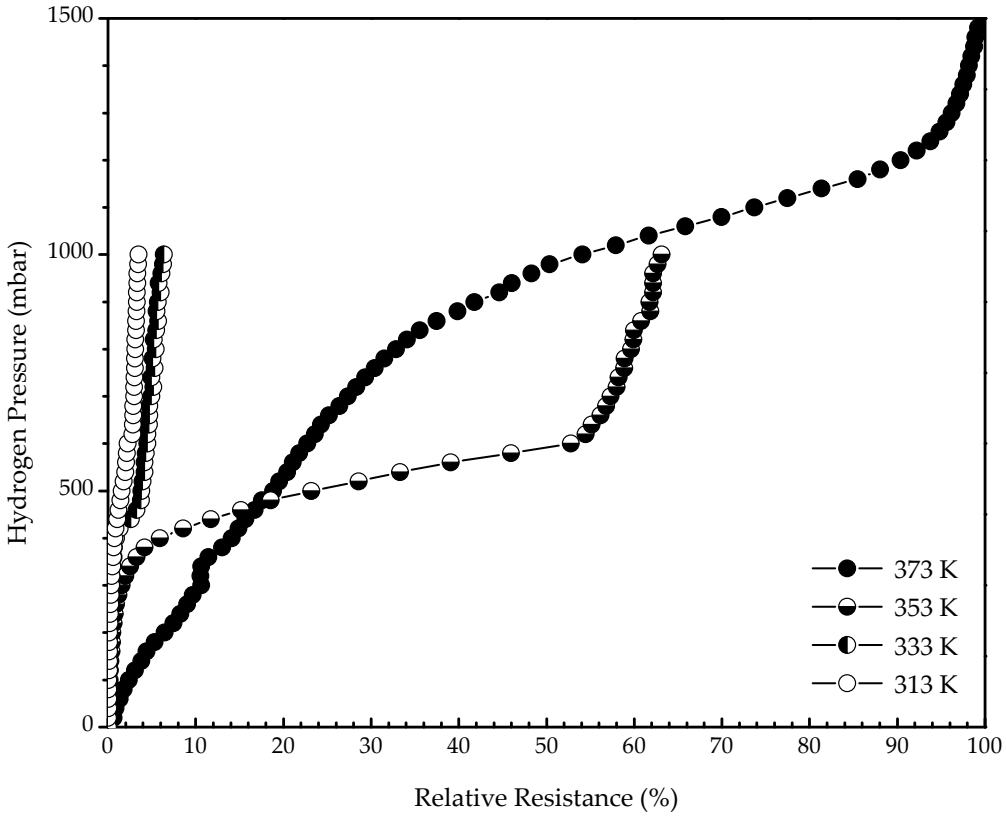

Figure 4.10 Hydrogen pressure vs. resistance curves of Mg/15 nm Pd thin films hydrogenated isothermally at temperatures 313, 333, 353 and 373 K.

It is clearly seen that isothermal hydrogenations at 313, 333 and 353 K start in the vicinity of 0.4 bar. The total hydrogen uptakes are, however, small for 313 and 333 K. Here, hydrogen uptake at 353 K is quite remarkable with approximately 62% change in its resistance. The uptake saturated at 0.6 bar for this sample, i.e. higher hydrogen pressures did not lead to a further increase in film resistance. Isothermal hydrogenation at a higher temperature, i.e. 373 K, on the other hand, exhibited a somewhat different behavior than the previous. For this sample, hydrogen uptake did not reach to saturation until 1.25 bar, but eventually resulted in the highest uptake. Here, the hydrogen uptake increased with increasing temperature.

Optical transmittance spectra of the hydrogenated thin films are shown in Figure 4.11. These data verify the resistance measurements by showing that the hydrogenation at higher temperatures (353 and 373 K) leads to a higher increase in transmittance, i.e. a higher amount of MgH_2 formed in the sample.

X-ray diffraction profiles of the current films hydrogenated at 313, 333, 353 and 373 K are given in Figure 4.12. It is seen that the MgH_2 has been formed in all cases, producing (110), (101), (200) and (211) reflections in general. Here, hydrogenation at 313 K differs from the others; only the (110) and (101) reflections of the hydride phase are seen in its diffractogram. According to the x-ray diffraction patterns, only the one at 353 K resulted in full hydrogenation, i.e. all Mg has been transformed into MgH_2. It is also worth mentioning that isothermal hydrogenations at 313 and 353 K were much more successful than the hydrogenations at 333 and 373 K, respectively, in terms of the fractions transformed. This finding, then, invalidated the previous results obtained by electrical resistance and optical transmittance measurements. Such a discrepancy has appeared presumably due to the negative contribution of Pd overlayer as already discussed in detail in the previous section.

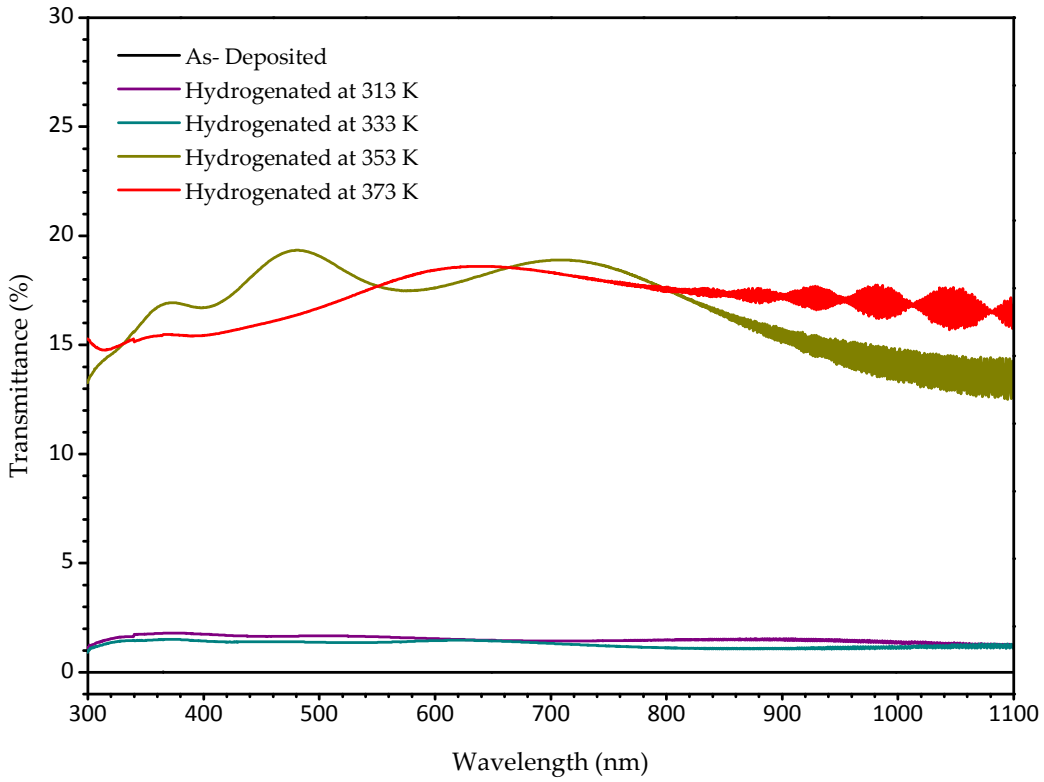

Figure 4.11 Optical transmittance spectra of 350 nm Mg/15 nm Pd thin films hydrogenated isothermally at temperatures 313, 333, 353 and 373 K. Transmittance spectrum of the as-deposited sample is also given for reference.

In order to study the effect of pressure on isothermal loading behaviors of Pd-covered Mg thin films, samples were loaded at much lower hydrogen pressures for extended exposure times. In the first experiment, hydrogen loading was carried out at 393 K under 0.2 bar pressure for 10 hours. X-ray diffraction profile obtained for this sample is given in Figure 4.13(a). It is seen that the greater portion of Mg has been transformed into MgH_2, producing (110), (101) and (200) reflections. However, (002) reflection that belong to Mg is still present – yet with a reduced intensity – indicating that the sample did not fully transform into magnesium hydride.

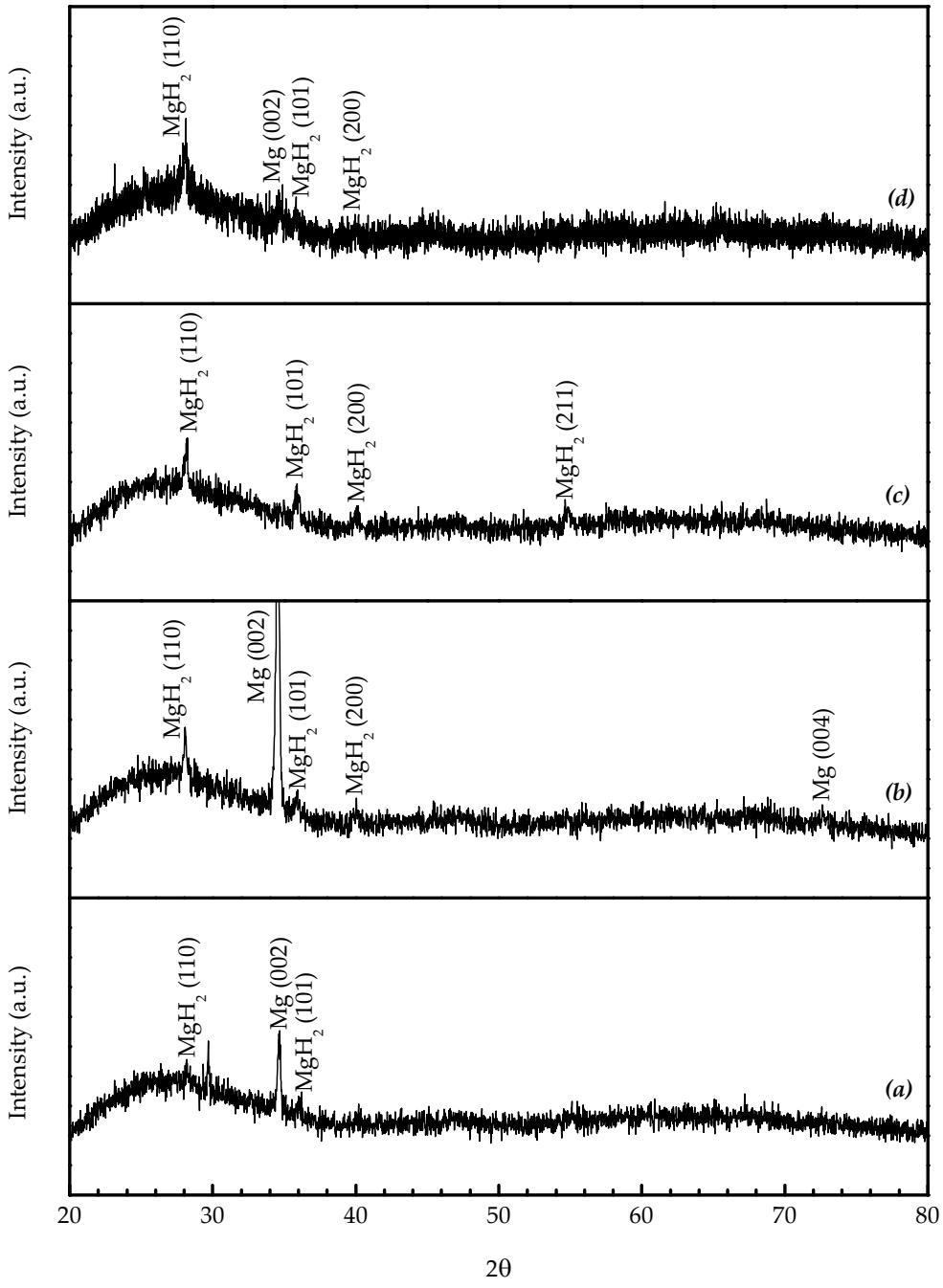

Figure 4.12 X-ray diffraction profiles of 350 nm Mg/15 nm Pd thin films hydrogenated isothermally at temperatures (a) 313, (b) 333, (c) 353 and (d) 373 K.

In another experiment again conducted at 393 K, the sample was exposed to 0.01 bar hydrogen gas for 80 hours. X-ray diffraction profile of this sample is shown in Figure 4.13(b). Only the (110), (101) and (200) peaks of MgH_2 are seen, showing that the sample is fully transformed into MgH_2. Therefore, it can be concluded that it is possible to obtain fully hydrogenated thin films by isothermal loading under hydrogen pressures as low as 0.01 bar. However, since the reaction kinetics strongly depend on the hydrogenation pressure, temperature and exposure time must be well-adjusted; i.e. exposure duration must be extended for low-pressure hydrogenation.

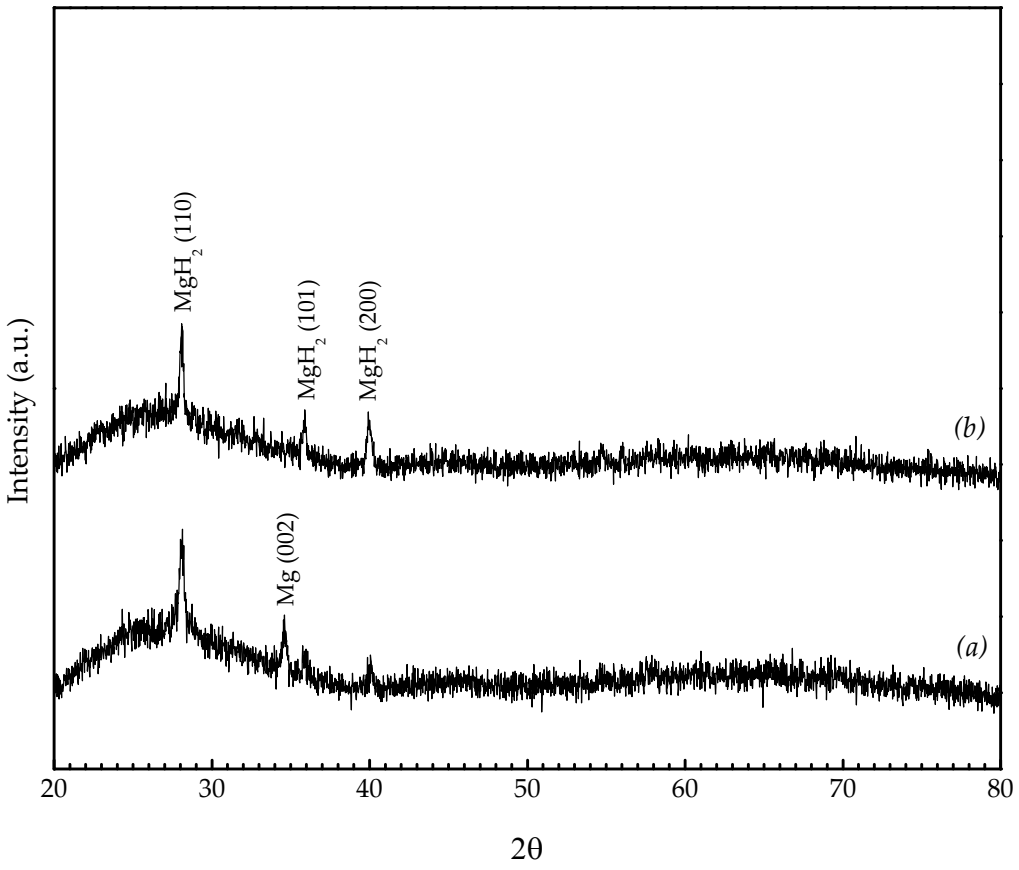

Figure 4.13 X-ray diffraction profiles of 350 nm Mg/11 nm Pd thin films hydrogenated isothermally at 393 K; (a) under 0.2 bar for 10 hours, (b) under 0.01 bar for 80 hours.

4.3.2 Isochronal Hydrogenation of Magnesium Thin Films

In order to determine the hydrogenation temperatures, Mg and Pd-covered Mg thin films were exposed to hydrogen gas at various pressures; i.e. 0.1, 0.5, 1 or 10 bar, under isochronal conditions. X-ray diffraction profiles obtained for 350 nm thick pure magnesium thin films isochronally hydrogenated up to 453 K are given in Figure 4.14. There is no sign of MgH_2 phase in none of these diffractograms, implying that pure magnesium films do not react with hydrogen under the given conditions. This is plausible, as it is known that there is a significant activation barrier for hydrogen dissociation on clean magnesium surfaces (Nørskov *et al.*, 1981; Johansson *et al.*, 2006).

Moreover, formation of a thin blocking oxide layer at the surface might be responsible from this behavior; considering that these thin film samples were transferred from deposition chamber to the resistance measurement set-up without any special handling. It is well-known that magnesium is very reactive to oxygen and therefore exposure to air certainly starts a fast oxidation reaction at the surface.

Since x-ray diffraction patterns show no evidence for the formation of neither hydride nor oxide phases, it is not irrational to assume a very thin oxide layer at the magnesium surface. Despite of its negligible thickness, this layer probably blocks further oxygen diffusion and somehow preserves the underlying magnesium lattice. Such an oxide layer on magnesium generally behaves like a barrier to hydrogen absorption by preventing the access of hydrogen to metallic magnesium as emphasized by Hjort *et al.* (1996b).

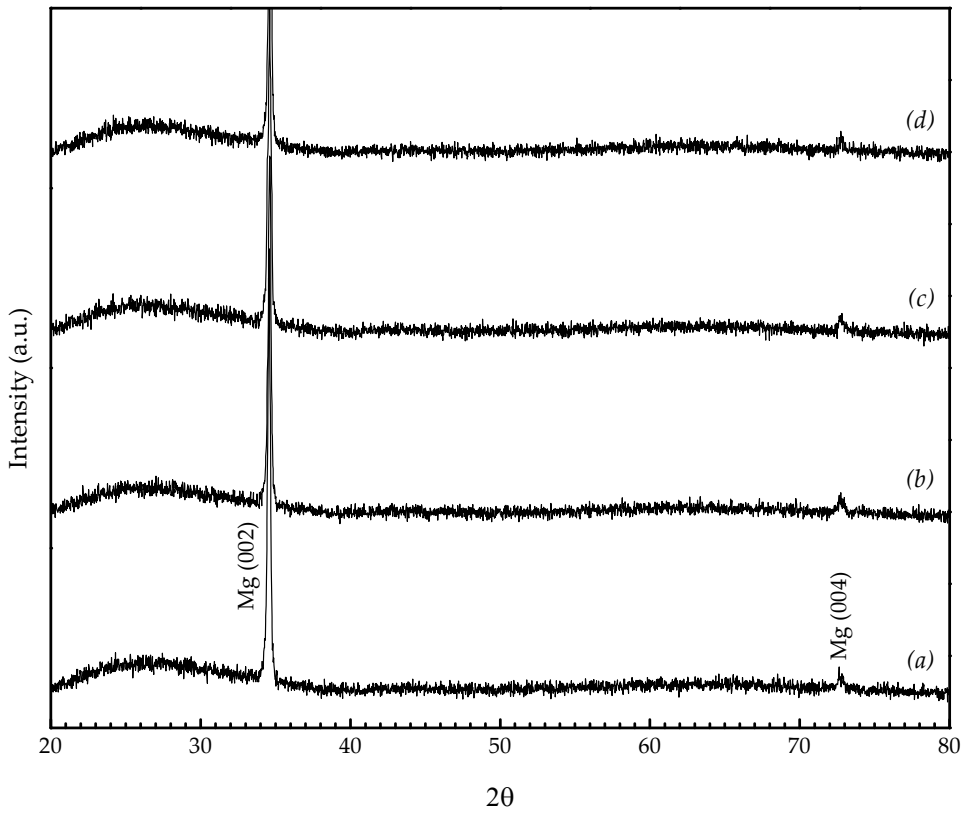

Figure 4.14 X-ray diffraction profiles of 350 nm thick pure Mg films exposed to hydrogen gas at pressures (a) 0.1, (b) 0.5, (c) 1 and (d) 10 bar.

Palladium cap layers (thicknesses ranging from 6 to 48 nm) were deposited on magnesium thin films in order to enhance hydrogen absorption by promoting H_2 dissociation as well as to protect the underlying film against oxidation. The deposited Pd-covered Mg thin films, therefore, possess the surface characteristics of palladium together with the bulk properties of magnesium. This was first proposed for bulk niobium by Pick *et al.* (1979) and then applied to magnesium thin films by Krozer and Kasemo (1987). Here, the catalytic effect of palladium cap layer can be explained in terms of its high sticking coefficient, i.e. low activation energy required for the dissociation of molecular hydrogen, as well as fast hydrogen diffusion in palladium towards the underlying magnesium layer.

The isochronal hydrogenation behaviors of Pd-covered 350 nm thick Mg thin films were followed by in situ resistance measurements. Whenever the loss of good electrical contact resulted in anomaly of the measured resistance value, inconsistent data were excluded.

Here, the procedure followed will be explained through a specific sample; 350 nm thick Mg thin film with 6 nm Pd overlayer. The volume fraction transformed, i.e. volume fraction hydrogenated, versus time (or temperature) graph of this sample hydrogenated isochronally up to 453 K under 1 bar hydrogen pressure is given in Figure 4.15. In this graph, the y-axis refers to "volume fraction transformed" as calculated from "% resistance change". Here, this calculation was carried out by using the equation of the linear fit given in Figure 4.9(a) on page 46. Hydrogenation temperature of this sample under 1 bar hydrogen pressure was determined to be 413 K from Figure 4.15 by simply reading the temperature corresponding to the half maximum of the vertical uptake line.

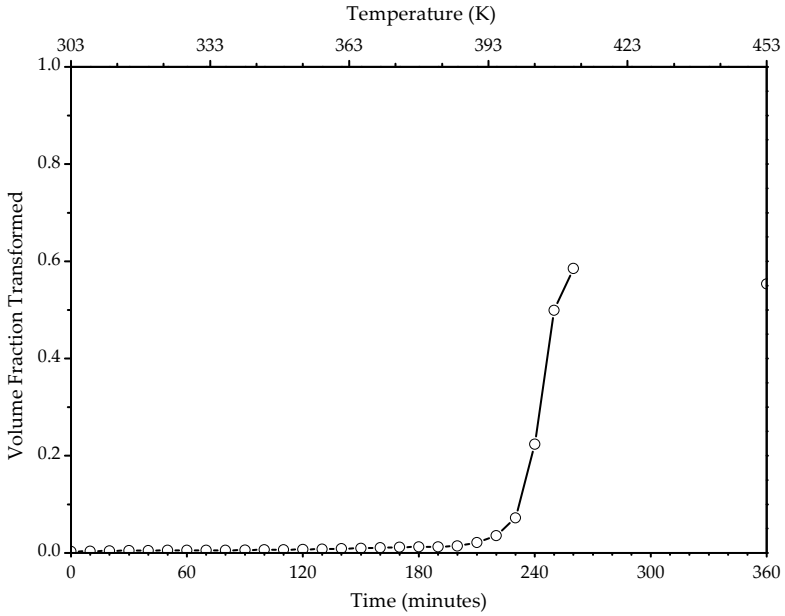

Figure 4.15 Volume fraction transformed vs. time (or temperature) graph of a 350 nm Mg thin film with 6 nm Pd overlayer, hydrogenated under 1 bar pressure.

SEM surface image of the same sample after isochronal hydrogenation under 1 bar pressure for 6 hours is given in Figure 4.16, revealing the hydrogen-induced morphological changes occurring in the thin film. See also Figure 4.4 on page 39 for comparison.

Figure 4.17, Figure 4.18, Figure 4.19 and Figure 4.20 show volume fraction transformed, i.e. volume fraction hydrogenated, versus time (or temperature) graphs of Pd-covered Mg thin films hydrogenated at 0.1, 0.5, 1 and 10 bar pressure, respectively. Hydrogenation temperatures as deduced from these plots are summarized in Table 4.2. It is seen that hydrogenation temperatures of Mg films with different Pd thicknesses loaded under isochronal conditions are in the range of 381-443 K.

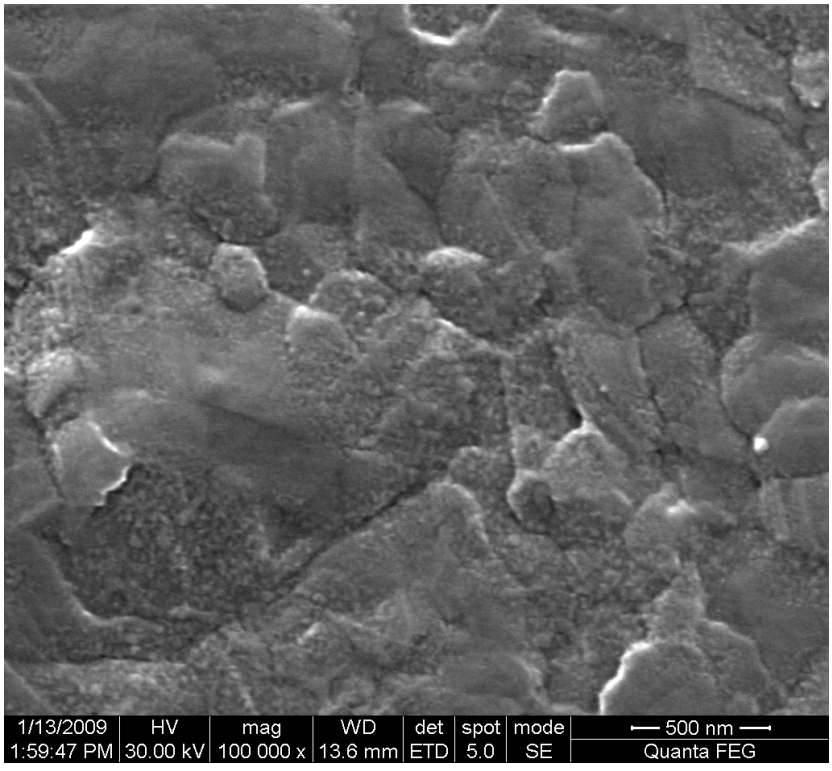

Figure 4.16 SEM surface image of a 350 nm Mg/6 nm Pd thin film hydrogenated (1 bar) under isochronal conditions.

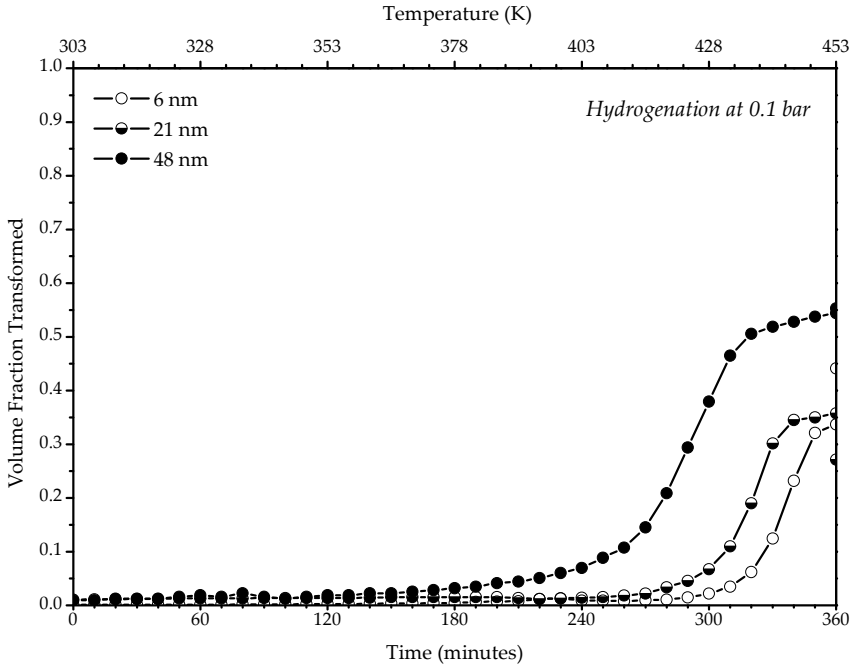

Figure 4.17 Volume fraction transformed vs. time (or temperature) graphs of 350 nm Mg thin films hydrogenated at 0.1 bar pressure for Pd overlayer thicknesses of 6, 21 and 48 nm.

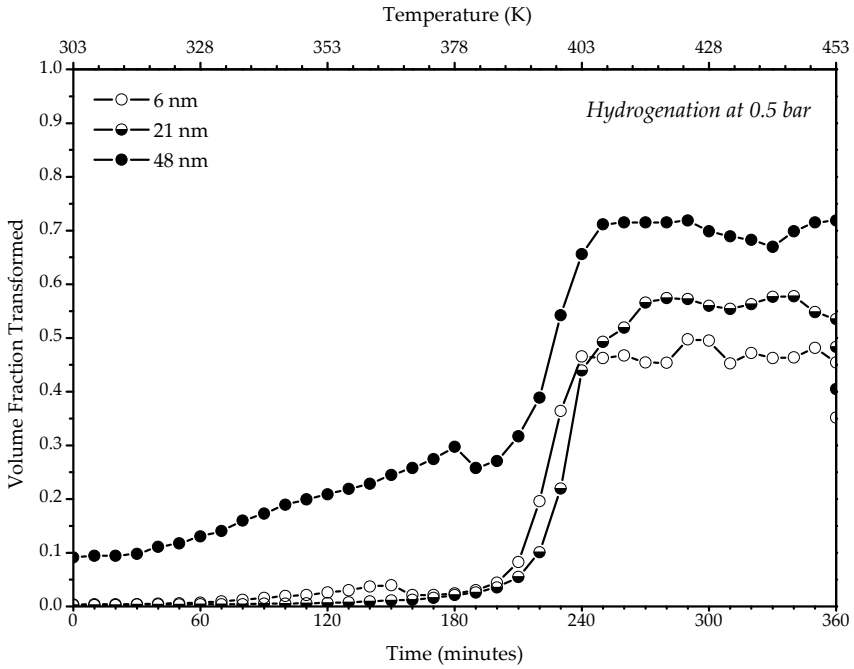

Figure 4.18 Volume fraction transformed vs. time (or temperature) graphs of 350 nm Mg thin films hydrogenated at 0.5 bar pressure for Pd overlayer thicknesses of 6, 21 and 48 nm.

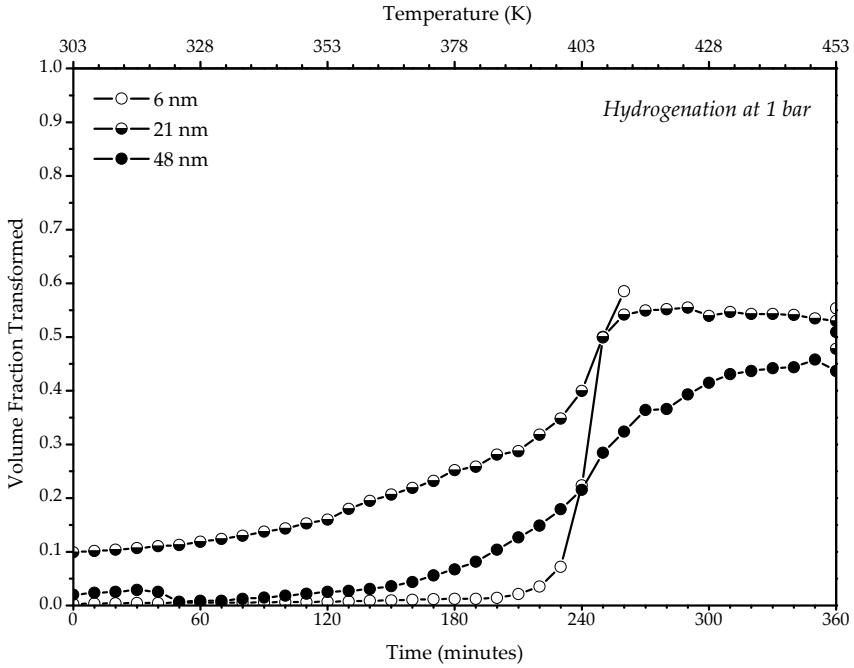

Figure 4.19 Volume fraction transformed vs. time (or temperature) graphs of 350 nm Mg thin films hydrogenated at 1 bar pressure for Pd overlayer thicknesses of 6, 21 and 48 nm.

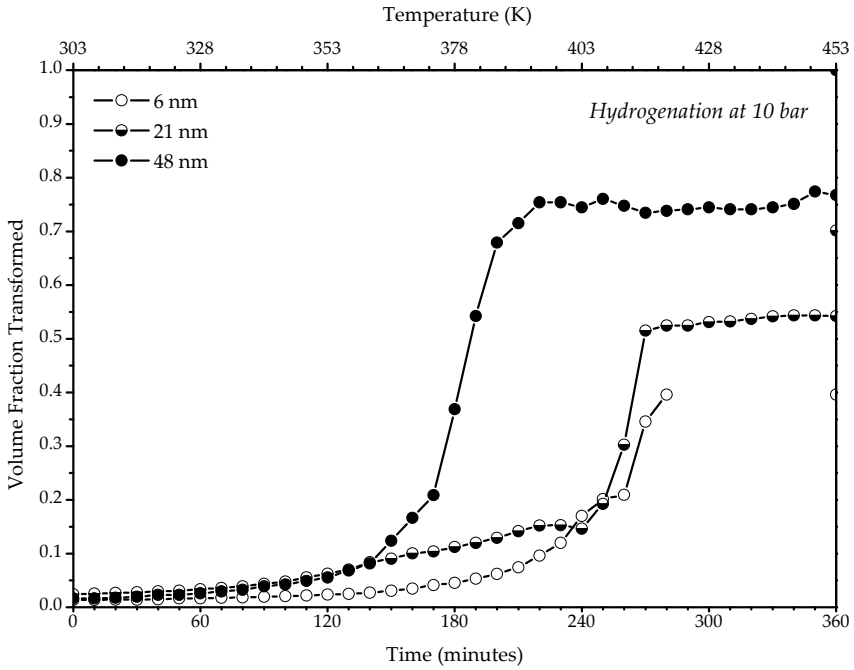

Figure 4.20 Volume fraction transformed vs. time (or temperature) graphs of 350 nm Mg thin films hydrogenated at 10 bar pressure for Pd overlayer thicknesses of 6, 21 and 48 nm.

Table 4.2 Hydrogenation temperatures deduced from Figure 4.17 to Figure 4.20 for Pd-covered Mg thin films hydrogenated at 0.1, 0.5, 1 and 10 bar pressure, respectively.

Hydrogenation Pressure (bar)	*Palladium Thickness (nm)*	*Hydrogenation Temperature (K)*
0.1	*6*	*443*
	21	*436*
	48	*425*
0.5	*6*	*398*
	21	*396*
	48	*393*
1	*6*	*413*
	21	*401*
	48	*404*
10	*6*	*421*
	21	*409*
	48	*381*

The variation of the hydrogenation temperature with the applied pressure is not exactly reproducible, though the temperature is always in this reported range. Here, one of the most striking observations is that the hydrogenation temperature strictly depends on Pd overlayer thickness in the case of high pressure hydrogenation (see Figure 4.20 on page 58). In order to clearly demonstrate this behavior, hydrogenation temperatures were plotted as a function of palladium overlayer thickness, as shown in Figure 4.21. It is seen that as the thickness of the Pd overlayer increases hydrogenation temperature decreases for all pressures, for thicknesses up to 20 nm. Here, only the variation of temperature with Pd overlayer thickness in the case of hydrogenation under 10 bar pressure is noteworthy, indicating a strong dependence.

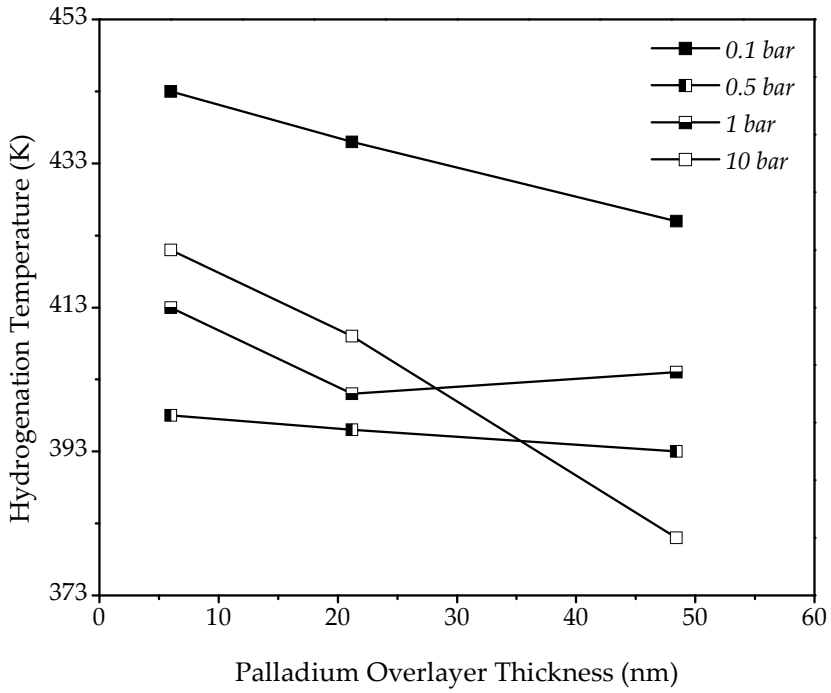

Figure 4.21 Variation of hydrogenation temperature with palladium overlayer thickness.

X-ray diffraction profiles of Pd-covered Mg thin film samples hydrogenated at 0.1, 0.5 and 1 bar pressure are given in Figure 4.22, Figure 4.23 and Figure 4.24, respectively. As the samples react with hydrogen, (110) and (101) reflections of the MgH_2 phase start to appear. However, reflections that belong to Mg are still present – yet with a reduced intensity – indicating that samples did not fully transform into magnesium hydride. For the samples hydrogenated under 10 bar pressure, on the other hand, only (110) and (220) reflections belonging to MgH_2 are seen (see Figure 4.25), implying preferred orientation of the nucleating hydride phase along this direction. It should be also emphasized that within all the samples studied here, only the 350 nm thick Mg thin film covered with 48 nm Pd was fully transformed into magnesium hydride upon hydrogenation under 10 bar. Since the concentration of dissolved hydrogen in metals increases with increasing hydrogen pressure according to the well-known Sievert's law, it is plausible that films exhibit fast kinetics and larger hydrogen uptakes at 10 bar hydrogen pressure.

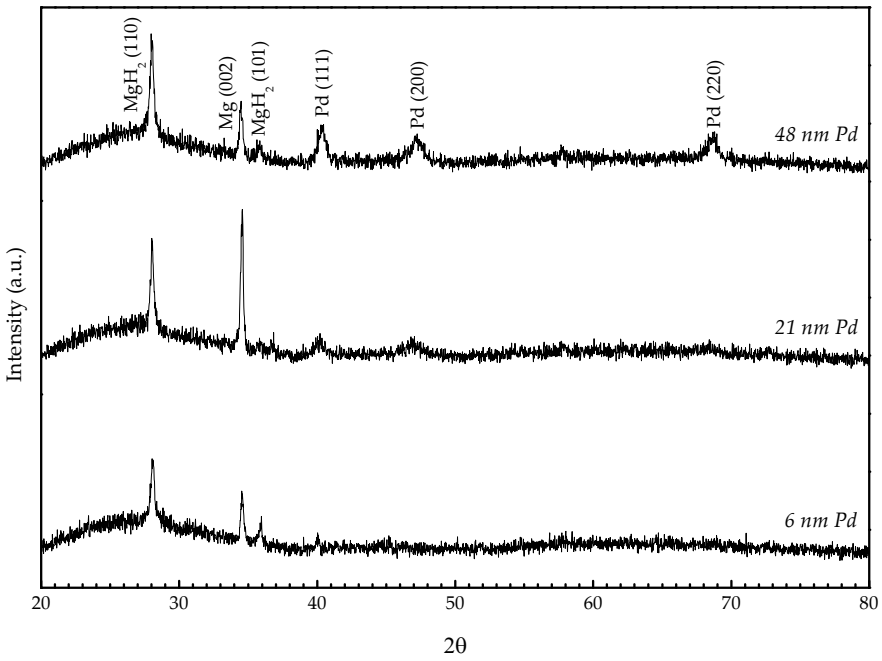

Figure 4.22 X-ray diffraction profiles of Pd-covered 350 nm thick Mg thin films hydrogenated under 0.1 bar pressure.

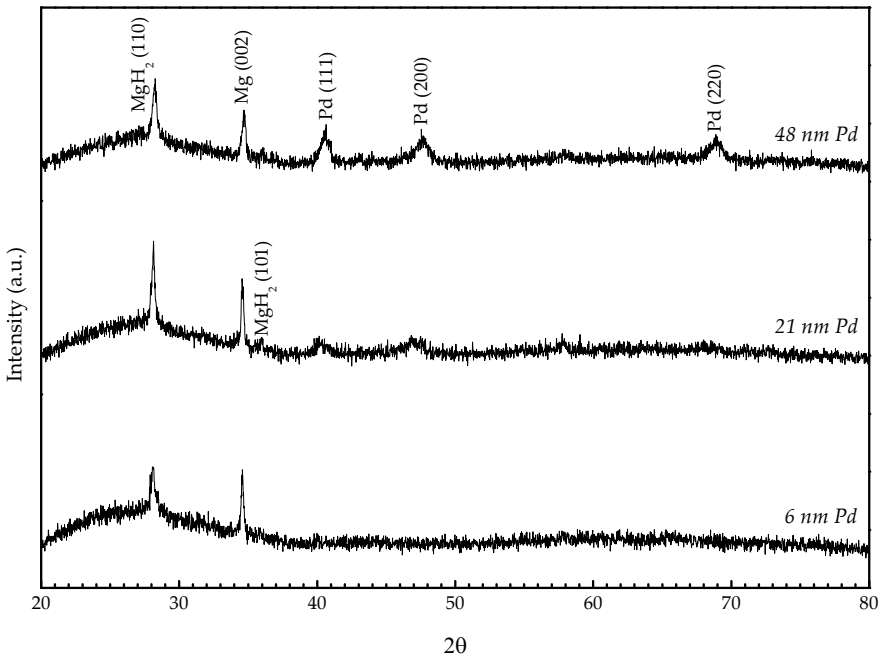

Figure 4.23 X-ray diffraction profiles of Pd-covered 350 nm thick Mg thin films hydrogenated under 0.5 bar pressure.

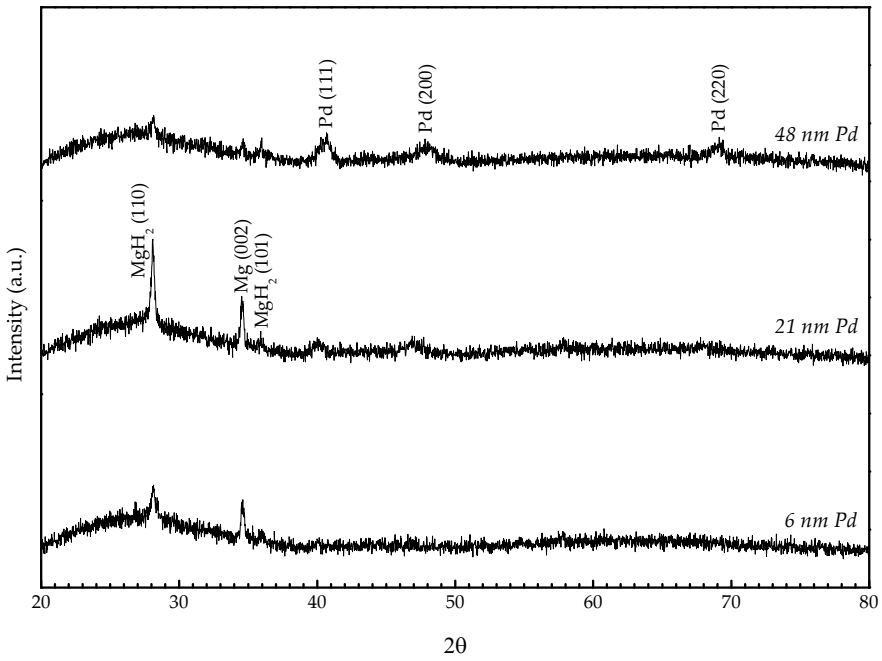

Figure 4.24 X-ray diffraction profiles of Pd-covered 350 nm thick Mg thin films hydrogenated under 1 bar pressure.

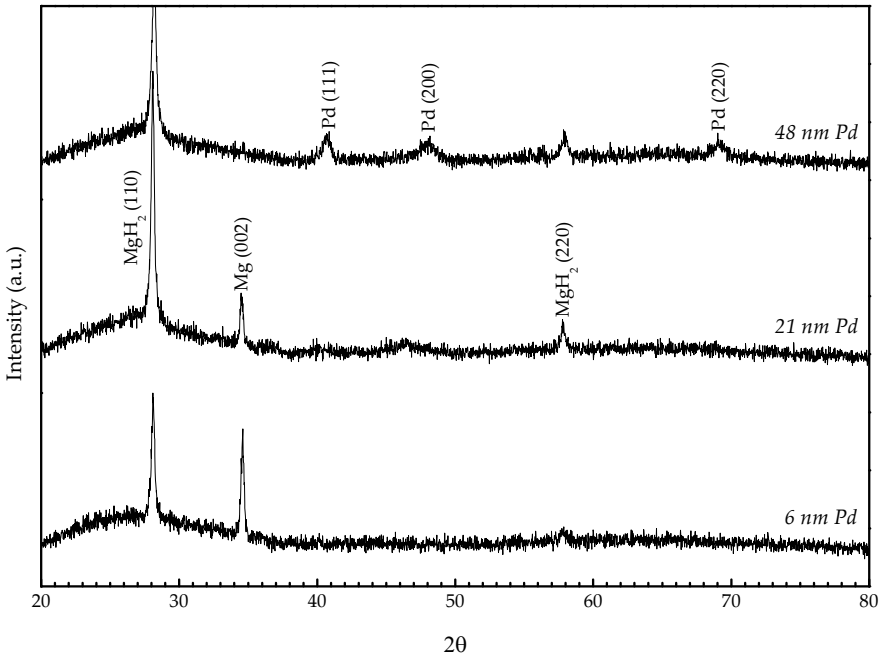

Figure 4.25 X-ray diffraction profiles of Pd-covered 350 nm thick Mg thin films hydrogenated under 10 bar pressure.

4.3.3 Isothermal vs. Isochronal Hydrogenation

Representative x-ray diffraction patterns of Pd-covered Mg thin film samples hydrogenated under isothermal and isochronal conditions are given in Figure 4.26(a) and (b), respectively. After an isothermal hydrogenation at 353 K under pressures up to 1 bar, the hydride phase forms with a random texture, i.e. (110), (101), (200) and (211) reflections of MgH_2 are observed.

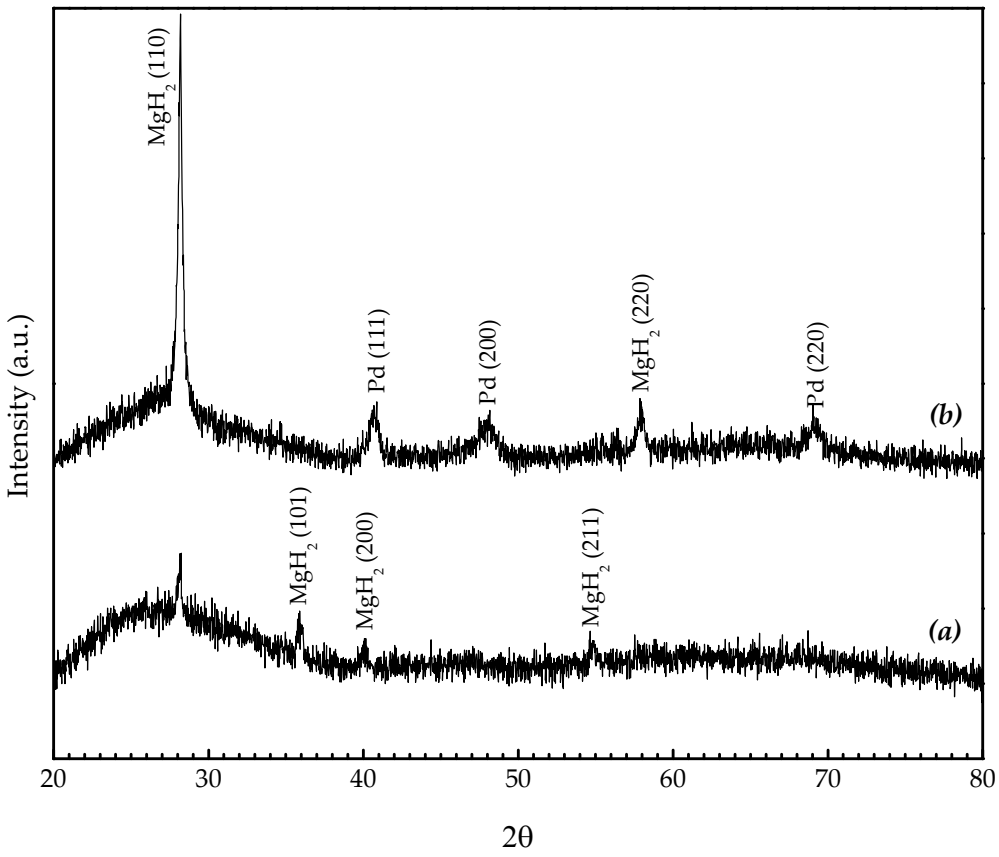

Figure 4.26 X-ray diffraction profiles of Pd-covered Mg thin films; (a) after isothermal hydrogenation (353 K) up to 1 bar, and (b) after isochronal hydrogenation (10 bar) up to 453 K.

For the samples hydrogenated via isochronal route, on the other hand, two peaks of MgH_2 were observed in general; (110) and (101), the former being far more dominant. It should be emphasized that MgH_2 occurring mainly with (110) reflection implies a textured structure. Figure 4.26(b) shows such an example where especially under 10 bar hydrogen pressure MgH_2 forms with (110) // glass substrate. The reflections belonging to Pd are more apparent in this diffractogram due to the much thicker Pd overlayer deposited on this sample, i.e. 15 vs. 48 nm.

Among all the samples studied here, only one showed an opposite behavior than that reported above. The diffractogram obtained for that sample has already been given in Figure 4.12(a) on page 51. Only (110) and (101) peaks of MgH_2 phase are seen here, although the hydrogenation was carried out under an isothermal condition. This is plausible since the hydrogenation temperature in this experiment, i.e. 313 K, is rather low, resembling the early stages of isochronal hydrogenation.

According to Schöber (1981), Mg to MgH_2 transformation follows the relationship Mg (001) // MgH_2 (100) and Mg [110] // MgH_2 [001]. According to this orientation relation, since as-deposited film has (001) texture, i.e. basal plane // glass substrate, the hydrogenated film is expected to develop MgH_2 (100) texture. This, however, is not the case. A schematic representation of this orientation relationship has been already given in Figure 2.2 on page 11. As shown by Schöber (1981), atomic displacements in Mg to MgH_2 transformation is rather small giving rise to contractions of 13.6% and 6% along the [100] and [001] directions in MgH_2, respectively. If MgH_2 were to be formed with (100) texture, then this would lead to 13.6% contraction in the through thickness direction. Since Mg to MgH_2 accompanies a substantial volume expansion of 32.57%, such a transformation would lead to a severe in-plane lattice mismatch.

The accommodation of in-plane lattice mismatch would be difficult in thin films due to their geometry. In this respect, the easiest direction which could tolerate such a distortion would be the through thickness direction. According to current observation, Mg to MgH_2 transformation converts Mg (001) to mainly MgH_2 (110). Such a relationship has also been reported by Bokhonov *et al.* (1987) for Mg single crystals and whiskers. The schematic representation of this conversion is given in Figure 4.27, where Mg (001)[100] // MgH_2 (110)[001]. Here, the lattice mismatch, as reported by Kelekar *et al.* (2007), is highest in the through thickness direction. As could be verified in Figure 4.27, this transformation leads to a through thickness lattice expansion of 22.58%, leaving a very little distortion for the in-plane accommodation of volume expansion.

The (110) texture in MgH_2 is mostly accompanied with a weak (101) component. This implies that a certain fraction of Mg (001) is converted to MgH_2 (101). Schematic representations of this transformation are shown in Figure 4.28 and Figure 4.29, respectively. Here, it appears that the lattices have relatively good match when Mg [210] // MgH_2 [-101]. Calculations show that, for this case, the lattice contracts by 3.64% along the thickness direction, a value which is intermediate between those for Mg (001) // MgH_2 (100) and Mg (001) // MgH_2 (110). This implies that in-plane distortion for Mg (001)[210] // MgH_2 (101)[-101] is also intermediate between the two.

Distortions as they occur in the above transformations can be represented by assuming a spherical volume element of Mg. Upon hydrogenation, spherical Mg transforms into an ellipsoidal MgH_2 as a result of the distortions produced along the x-, y- and z-axes. This is demonstrated for Mg (001) // MgH_2 (100), Mg (001) // MgH_2 (110) and Mg (001) // MgH_2 (101) transformations in Figure 4.30(a), (b) and (c), respectively.

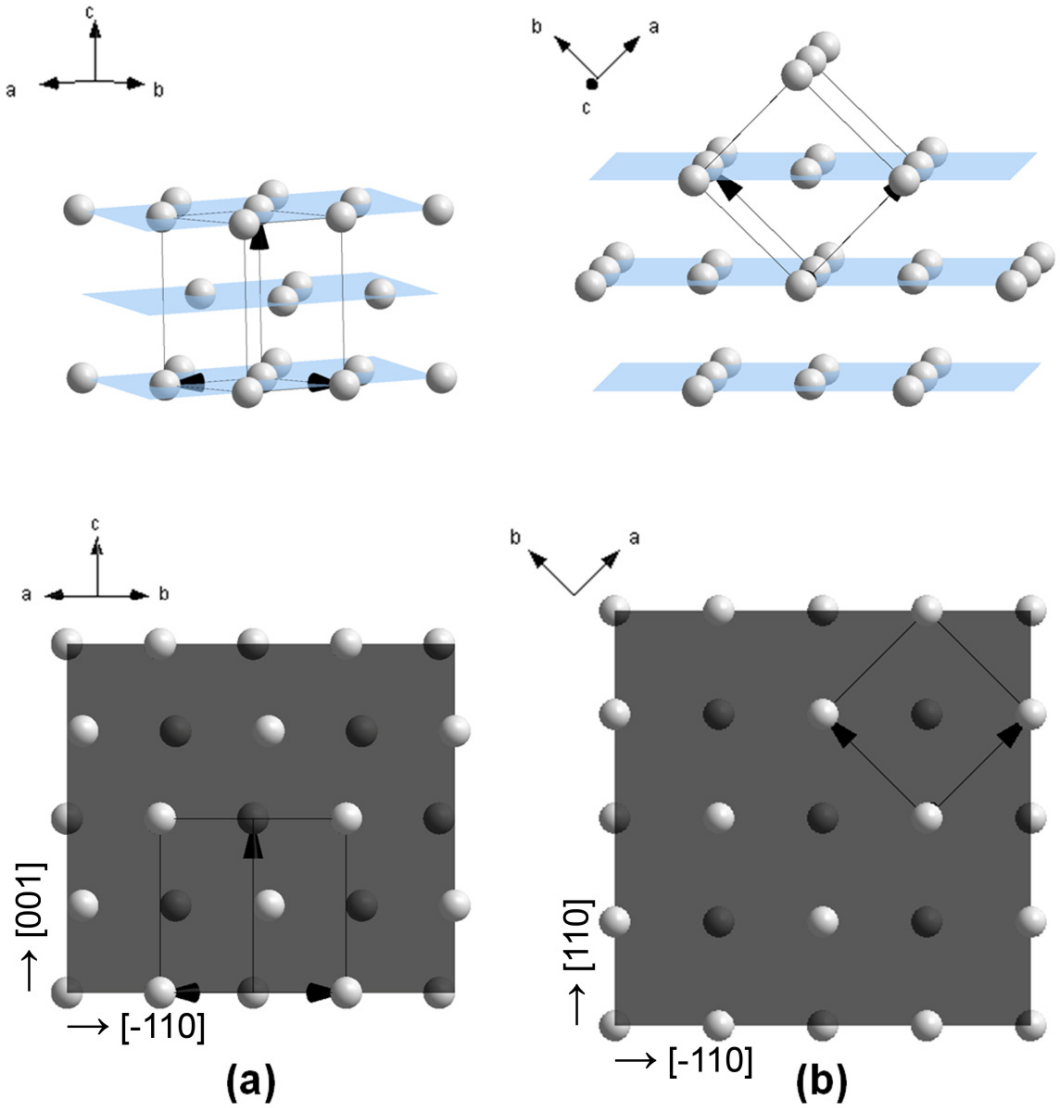

Figure 4.27 The schematic representation of Mg to MgH_2 transformation with Mg (001)[100] // MgH_2 (110)[001]; (a) Mg crystal, paper-plane (110), (b) MgH_2 crystal, paper-plane (001) (only Mg atoms are shown). Drawings above the figures refer to the same crystals tilted slightly to display the respective planes, i.e. Mg (001) and MgH_2 (110). This transformation leads to lattice expansion of 22.58% along the through thickness direction.

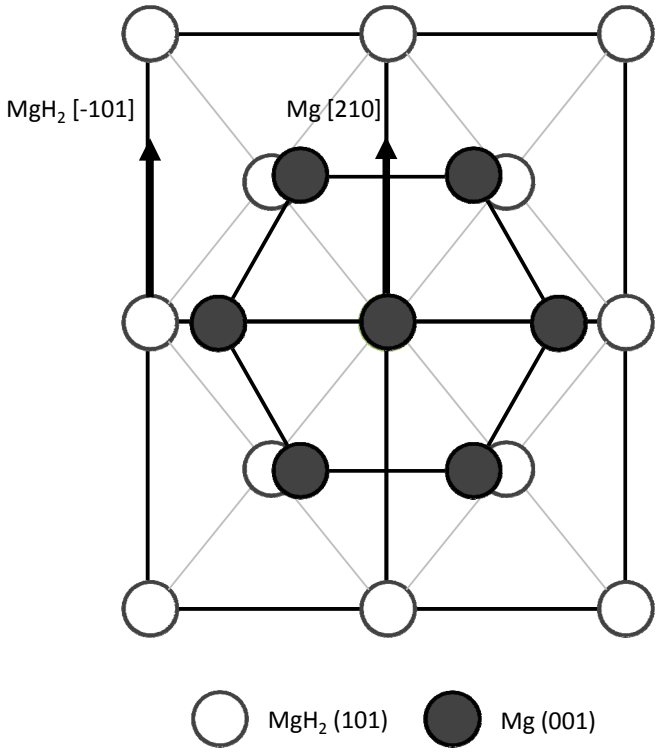

Figure 4.28 Schematic representation of atomic displacements associated with the Mg (001) // MgH_2 (101) and Mg [210] // MgH_2 [-101] orientation relation of transformation (only the Mg atoms are shown).

Observation reported above implies that Mg to MgH_2 transformation follows different routes depending on the type of hydrogen loading. Isothermal loading would lead to a prolific nucleation in a variety of orientations. However, the case of isochronal hydrogenation is different. This type of loading would be expected to favor the growth of MgH_2 phase as they first nucleate. It appears that among the various Mg to MgH_2 transformations, the nuclei which form first are those that minimize the in-plane lattice distortion. Thus, for the current case of strongly (001) textured Mg, the transformation selected is Mg (001)[100] // MgH_2 (110)[001]. Even though the in-plane lattice mismatch is relatively small, still with the progress of hydrogenation, the distortion builds up which leads to morphological changes as well as to formation of microcracks.

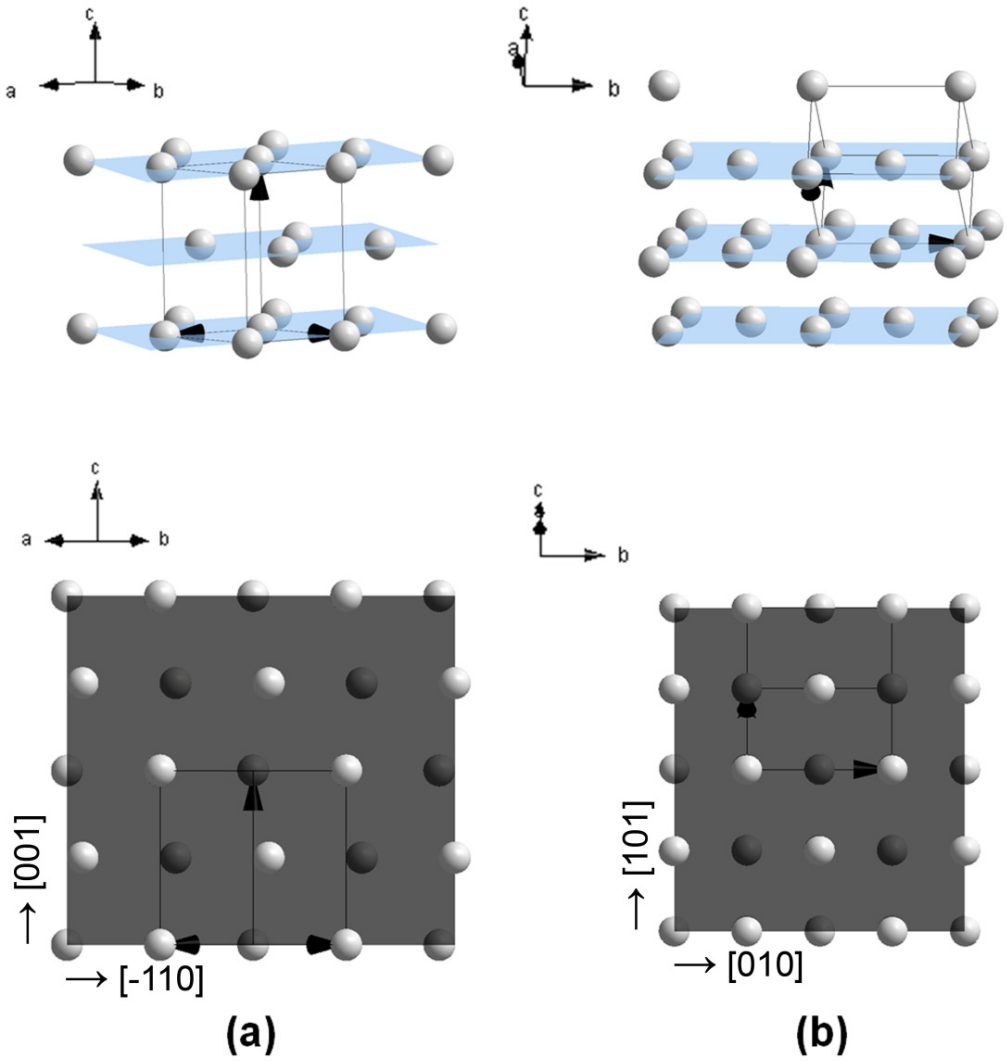

Figure 4.29 The schematic representation of Mg to MgH_2 transformation with Mg (001)[210] // MgH_2 (101)[-101]; (a) Mg crystal, paper-plane (110), (b) MgH_2 crystal, paper-plane (-101) (only Mg atoms are shown). Drawings above the figures refer to the same crystals tilted slightly to display the respective planes, i.e. Mg (001) and MgH_2 (101). This transformation leads to lattice contraction of 3.64% along the through thickness direction.

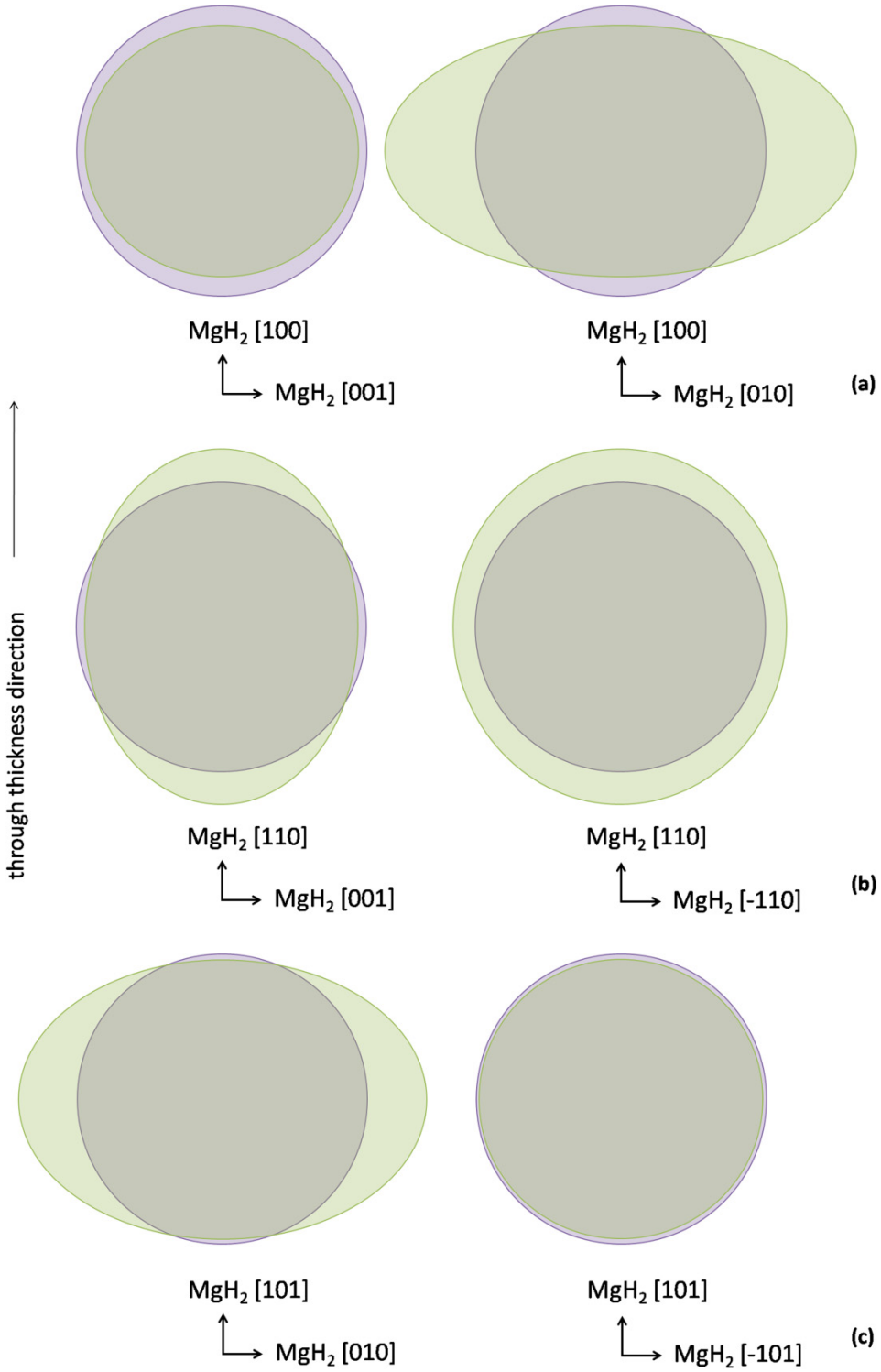

Figure 4.30 Distortions produced along the x-, y- and z-axes for (a) Mg (001) // MgH_2 (100), (b) Mg (001) // MgH_2 (110) and (c) Mg (001) // MgH_2 (101) transformations. Green and purple regions correspond to MgH_2 and Mg phases, respectively.

CHAPTER 5

CONCLUSIONS

In this study, pure and palladium-covered 350 nm thick magnesium thin films were deposited on glass substrates via thermal evaporation. The hydrogenation behaviors of these films were studied with a purpose built set-up for resistance measurements. The aspects of hydrogenation were also followed by optical transmittance measurements and x-ray diffraction studies. A comparative study was presented, in which the data obtained from two-point probe electrical resistance and optical transmittance measurement techniques have been questioned in terms of how well they represent the amount of MgH_2 formed in the samples. Results showed that both techniques provide fast and reliable measure with regard to hydrogenation behaviors of the Mg thin films.

Films in the as-deposited state were highly textured with Mg (001) parallel to the substrate. Hydrogen loading experiments on these films were carried out in two different conditions; namely isothermal and isochronal. Isothermal hydrogenation experiments conducted on Pd-covered Mg thin films have revealed that these films can absorb hydrogen at temperatures starting from 333 K, producing MgH_2 with a random texture. When the films were heated slowly starting from the room temperature, on the other hand, hydrogenation gives rise to a textured MgH_2, where (110) parallel to the substrate with a minor (101) component. The origin of this behavior was explained in terms of different routes

followed in Mg to MgH_2 transformation depending on the type of hydrogen loading; i.e. isothermal loading leads to a prolific nucleation which favors random texture, whereas isochronal loading favors the growth of MgH_2 phase as they first nucleate resulting in preferred orientation. It was further shown that the formation of this textured MgH_2 with isochronal loading is due to minimization of in-plane lattice distortion in Mg to MgH_2 transformation.

REFERENCES

Akyıldız H, Özenbaş M, Öztürk T, 2006, *"Hydrogen absorption in magnesium based crystalline thin films"*, Int. J. Hydrogen Energ. 31: 1379-1383.

Akyıldız H, 2009, *"Hydrogen Storage in Mg-Based Thin Films"*, unpublished research, Middle East Technical University, Turkey.

Ball P, 1998, *"Smart materials: Off and on reflection"*, Nature 391: 232-233.

Baybörü E, 2001, "*Mechanical Milling of Magnesium Powders and Measurement of their Hydrogen Sorption Characteristics"*, M.Sc. Thesis, Middle East Technical University, Turkey.

Bokhonov B, Ivanov E, Boldyrev V, 1987, *"A study of the electron-beam induced decomposition of magnesium hydride single crystals"*, Mater. Lett. 5 (5-6): 218-221.

Buschow KHJ, Bouten PCP, Miedema AR, 1982, *"Hydrides formed from intermetallic compounds of two transition metals: a special class of ternary alloys"*, Rep. Prog. Phys. 45: 937-1039.

Dam B, Gremaud R, Broedersz C, Griessen R, 2007, *"Combinatorial thin film methods for the search of new lightweight metal hydrides"*, Scripta Mater. 56: 853-858.

Domènech-Ferrer R, Sridharan MG, Garcia G, Pi F, Rodríguez-Viejo J, 2007, *"Hydrogenation properties of pure magnesium and magnesium-aluminium thin films"*, J. Power Sources 169: 117-122.

Ellinger FH, Holley CE Jr, McInteer BB, Pavone D, Potter RM, Staritzky E, Zachariasen WH, 1955, *"The preparation and some properties of magnesium hydride"*, J. Amer. Chem. Soc. 77 (9): 2647-2648.

Gremaud R, Broedersz CP, Borsa DM, Borgschulte A, Mauron P, Schreuders H, Rector JH, Dam B, Griessen R, 2007, *"Hydrogenography: An optical combinatorial method to find new light-weight hydrogen-storage materials"*, Adv. Mater. 19: 2813-2817.

Güvendiren M, 2003, *"Effects of Additives on Mechanical Milling and Hydrogenation of Magnesium Powders"*, M.Sc. Thesis, Middle East Technical University, Turkey.

Higuchi K, Kajioka H, Toiyama K, Fujii H, Orimo S, Kikuchi Y, 1999, *"In situ study of hydriding-dehydriding properties in some Pd/Mg thin films with different degree of Mg crystallization"*, J. Alloy. Compd. 293-295: 484-489.

Higuchi K, Yamamoto K, Kajioka H, Toiyama K, Honda M, Orimo S, Fujii H, 2002, *"Remarkable hydrogen storage properties in three-layered Pd/Mg/Pd thin films"*, J. Alloy. Comp. 330-332: 526-530.

Hjort P, Krozer A, Kasemo B, 1996a, *"Resistivity and hydrogen uptake measurements in evaporated Mg films at 350 K"*, J. Alloy. Compd. 234: L11-L15.

Hjort P, Krozer A, Kasemo B, 1996b, *"Hydrogen sorption kinetics in partly oxidized Mg films"*, J. Alloy. Compd. 237: 74-80.

Huiberts JN, Griessen R, Rector JH, Wijngaarden RJ, Dekker JP, de Groot DG, Koeman NJ, 1996a, *"Yttrium and lanthanum hydride films with switchable optical properties"*, Nature 380: 231-234.

Huiberts JN, Rector JH, Wijngaarden RJ, Jetten S, de Groot D, Dam B, Koeman NJ, Griessen R, Hjörvarsson B, Olafsson S, Cho YS, 1996b, *"Synthesis of yttriumtrihydride films for ex-situ measurements"*, J. Alloy. Compd. 239: 158-171.

Ingason AS and Olafsson S, 2005, *"Thermodynamics of hydrogen uptake in Mg films studied by resistance measurements"*, J. Alloy. Compd. 404-406: 469-472.

Ingason AS and Olafsson S, 2006, *"Influence of MgO nano-crystals on the thermodynamics, hydrogen uptake and kinetics in Mg films"*, Thin Solid Films 515: 708-711.

Isidorsson J, Giebels IAME, Arwin H, Griessen R, 2003, *"Optical properties of MgH_2 measured in situ by ellipsometry and spectrophotometry"*, Phys. Rev. B 68: 115112.

Ivey DG, Northwood DO, 1983, *"Storing energy in metal hydrides: A review of the physical metallurgy"*, J. Mater. Sci. 18: 321-347.

Jain IP, Vijay YK, Malhotra LK, Uppadhyay, 1988, *"Hydrogen storage in thin film metal hydride - A review"*, Int. J. Hydrogen Energ. 13 (1): 15-23.

Johansson M, Ostenfeld CW, Chorkendorff I, 2006, *"Adsorption of hydrogen on clean and modified magnesium films"*, Phys. Rev. B 74: 193408.

Kelekar R, Giffard H, Kelly ST, Clemens BM, 2007, *"Formation and dissociation of MgH_2 in epitaxial Mg thin films"*, J. Appl. Phys. 101: 114311.

Kremers M, Koeman NJ, Griessen R, Notten PHL, Tolboom R, Kelly PJ, Duine PA, 1998, *"Optical transmission spectroscopy of switchable yttrium hydride films"*, Phys. Rev. B 57 (8): 4943-4949.

Krozer A and Kasemo B, 1987, *"Unusual kinetics due to interface hydride formation in the hydriding of Pd/Mg sandwich layers"*, J. Vac. Sci. Technol. A 5 (4): 1003-1005.

Krozer A and Kasemo B, 1989, *"Equilibrium hydrogen uptake and associated kinetics for the Mg-H_2 system at low pressures"*, J. Phys-Condens. Mat. 1: 1533-1538.

Krozer A and Kasemo B, 1990, *"Hydrogen uptake by Pd-coated Mg: Absorption-decomposition isotherms and uptake kinetics"*, J. Less-Common Met. 160: 323-342.

Kumar S, Reddy GLN, Raju VS, 2008, *"Hydrogen storage in Pd capped thermally grown Mg films: studies by nuclear resonance reaction analysis"*, J. Alloy. Compd. *article in press*.

Léon A, Knystautas EJ, Huot J, Schulz R, 2002, *"Hydrogenation characteristics of air-exposed magnesium films"*, J. Alloy. Compd. 345: 158-166.

Léon A, Knystautas EJ, Huot J, Lo Russo S, Koch CH, Schulz R, 2003, *"Hydrogen sorption properties of vanadium- and palladium-implanted magnesium films"*, J. Alloy. Compd. 356-357: 530-535.

Liang G, Boily S, Huot J, Van Neste A, Schulz R, 1998, *"Mechanical alloying and hydrogen absorption properties of the Mg-Ni system"*, J. Alloy. Compd. 267: 302-306.

Liang G, Huot J, Boily S, Van Neste A, Schulz R, 1999, *"Hydrogen storage properties of nanocrystalline $Mg_{1.9}Ti_{0.1}Ni$ made by mechanical alloying"*, J. Alloy. Compd. 282: 286-290.

Nørskov JK, Houmøller A, Johansson PK, Lundqvist BI, 1981, *"Adsorption and dissociation of H_2 on Mg surfaces"*, Phys. Rev. Lett. 46 (4): 257-260.

Ostenfeld CW and Chorkendorff I, 2006, *"Effect of oxygen on the hydrogenation properties of magnesium films"*, Surf. Sci. 600: 1363-1368.

Ostenfeld CW, Johansson M, Chorkendorff I, 2007, *"Hydrogenation properties of catalyzed and non-catalyzed magnesium films"*, Surf. Sci. 601: 1862-1869.

Paillier J and Roué L, 2005, *"Hydrogen electrosorption and structural properties of nanostructured Pd-Mg thin films elaborated by pulsed laser deposition"*, J. Alloy. Compd. 404-406: 473-476.

Paillier J, Bouhtiyya S, Ross GG, Roué L, 2006, *"Influence of the deposition atmosphere on the characteristics of Pd-Mg thin films prepared by pulsed laser deposition"*, Thin Solid Films 500: 117-123.

Pasturel M, Slaman M, Schreuders H, Rector JH, Borsa DM, Dam B, Griessen R, 2006, *"Hydrogen absorption kinetics and optical properties of Pd-doped Mg thin films"*, J. Appl. Phys. 100: 023515.

Pick MA, Davenport JW, Strongin M, Dienes GJ, 1979, *"Enhancement of hydrogen uptake rates for Nb and Ta by thin surface overlayers"*, Phys. Rev. Lett. 43 (4): 286-289.

Qu J, Wang Y, Xie L, Zheng J, Liu Y, Li X, 2009, *"Superior hydrogen absorption and desorption behavior of Mg thin films"*, J. Power Sources 186: 515-520.

Richardson TJ, Slack JL, Armitage RD, Kostecki R, Farangis B, Rubin MD, 2001, *"Switchable mirrors based on nickel-magnesium films"*, Appl. Phys. Lett. 78 (20): 3047-3049.

Rydén J, Hjörvarsson B, Ericsson T, Karlsson E, Krozer A, Kasemo B, 1989, *"Unusual kinetics of hydride formation in Mg-Pd sandwiches, studied by hydrogen profiling and quartz crystal microbalance measurements"*, J. Less-Common Met. 152: 295-309.

Schöber T, 1981, *"The Magnesium-Hydrogen System: Transmission Electron Microscopy"*, Metall. Trans. A 12A (6): 951-957.

Shalaan E, Schmitt H, 2006, *"Mg nanoparticle switchable mirror films with improved absorption-desorption kinetics"*, Surf. Sci. 600 (18): 3650-3653.

Singh S, Eijt SWH, Zandbergen MW, Legerstee WJ, Svetchnikov VL, 2007, *"Nanoscale structure and the hydrogenation of Pd-capped magnesium thin films prepared by plasma sputter and pulsed laser deposition"*, J. Alloy. Compd. 441: 344-351.

Stander CM and Pacey RA, 1978, *"The lattice energy of magnesium hydride"*, J. Phys. Chem. Solids 39 (8): 829-832.

van der Sluis P, Ouwerkerk M, Duine PA, 1997, *"Optical switches based on magnesium lanthanide alloy hydrides"*, Appl. Phys. Lett. 70 (25): 3356-3358.

Vermeulen P, Graat PCJ, Wondergem HJ, Notten PHL, 2008, *"Crystal structures of Mg_yTi_{100-y} thin film alloys in the as-deposited and hydrogenated state"*, Int. J Hydrogen Energ. 33: 5646-5650.

Yamamoto K, Higuchi K, Kajioka H, Sumida H, Orimo S, Fujii H, 2002, *"Optical transmission of magnesium hydride thin film with characteristic nanostructure"*, J. Alloy. Compd. 330-332: 352-356.

Yoshimura K, Yamada Y, Okada M, 2004, *"Hydrogenation of Pd capped Mg thin films at room temperature"*, Surf. Sci. 566-568: 751-754.

Zachariasen WH, Holley CE Jr, Stamper JF Jr, 1963, *"Neutron diffraction study of magnesium deuteride"*, Acta Cryst. 16: 352-353.